24th August 2023 - Note added after first publication: This Supplementary Information file replaces that originally published 16th May 2023.

Electronic Supplementary Information

for

Cross-linkable, phosphobetaine-based, zwitterionic amphiphiles that form lyotropic bicontinuous cubic phases

Lauren N. Bodkin,[a] Zachary A. Krajnak,[a] Ruiqi Dong,[b] Chinedum O. Osuji[b] and Douglas L. Gin*[a]

[a] Department of Chemistry, University of Colorado, Boulder, CO 80309, USA. E-mail: douglas.gin@colorado.edu

[b] Department of Chemical and Biomolecular Engineering, University of Pennsylvania, Pennsylvania, PA 19104, USA.

Table of Contents

I.   Materials & General Procedures

Methyl gallate, ethylene glycol anhydrous (99.8%), and 2-hydroxy-2-methylpropiophenone (HMP, 97%) were purchased from Sigma-Aldrich. 11-Bromoundecan-1-ol, 2-chloro-2-oxo-1,3,2-dioxaphospholane (>95.0%), 1-methylpyrrolidine, 1,4-diazabicyclo[2.2.2] octane, and 4-dimethylaminopyridine were purchased from TCI America. Trimethylamine (1 M solution in THF, AcroSeal™) was purchased from VWR. Triethylamine (>99%), *N,N*-dimethylethylamine (99%), and *N,N*-dimethylhexylamine (98%) were purchased from Fisher Scientific. Silica gel (normal-

phase, 200 x 400 mesh) was purchased from Sorbent Technologies. Sodium hydroxide, sodium chloride, magnesium sulfate, sodium sulfate, Celite™ 545, Indicating Drierite® ($\geq$98% $CaSO_4$, <2% $CoCl_2$), and hydrochloric acid (all ACS Reagents) were purchased from Fisher Scientific and used as received. Acryloyl chloride, purchased from Sigma-Aldrich, was freshly distilled under Ar prior to use. 1,4-Dioxane, purchased from Sigma-Aldrich, was distilled from a sodium benzophenone ketyl before use. Triethylamine, purchased from Fisher Scientific, was distilled under Ar and stored in a Straus flask prior to use. All other chemicals and solvents were purchased from either Sigma-Aldrich, TCI America, or Fisher Scientific and used without further purification unless otherwise noted. All manipulations, except for reaction work-up procedures, were performed under air- and water-free conditions with light Ar flush using conventional Schlenk line techniques. Unless otherwise specified, organic extracts were dried over anhydrous sodium sulfate. Solvents were removed using a rotary evaporator, followed by drying on a Schlenk line ($\leq 10^{-4}$ torr). Non-sterile, hydrophilic poly(vinylidene fluoride) (PVDF) syringe filters (0.22-μm pore size, 13 mm) for the filtration of membrane casting solutions were purchased from Fisher Scientific. Poly(ether sulfone) (PES) ultraporous support membranes (0.03-μm, 47mm) for thin-film composite (TFC) membrane fabrication trials were purchased from Sterlitech.

II.   Instrumentation

^{1}H and ^{13}C NMR spectra were obtained using a Bruker AMX-300 (300 MHz for ^{1}H; 75 MHz for ^{13}C) spectrometer. Chemical shifts are reported in ppm relative to deuterated solvent. Fourier-transform infrared (FT-IR) spectroscopy measurements were performed using either a Thermo Scientific Nicolet 6700 spectrometer equipped with a PIKE MIRacle™ single-reflection horizontal attenuated total reflectance (ATR) accessory with a diamond crystal, an Agilent Cary 630 FT-IR instrument single-reflection horizontal ATR accessory with diamond crystal, or a JASCO 6300 instrument. Polarized light microscopy (PLM) studies were performed with a Leica DMRXP polarizing light microscope equipped with a Q-Imaging MicroPublisher 3.3 RTV digital camera, a Linkam LTS 350 thermal stage, and a Linkam CI 94 temperature controller. Lyotropic liquid-crystalline (LLC) mixtures were homogenized, as needed, using an IEC Centra-CL2 centrifuge. Powder X-ray diffraction (PXRD) spectra were obtained with an Inel CPS 120 diffraction system using monochromated Cu K_α radiation. This system was equipped with a holder to analyze film samples. All PXRD spectra were calibrated using a silver behenate diffraction standard (d_{100} = 58.4 $\pm$ 0.1 Å). PXRD measurements were all performed at ambient temperature (22 $\pm$ 1 °C). To help confirm/verify the bicontinuous cubic (Q) phase information provided by PXRD, small-angle X-ray scattering (SAXS) measurements were performed with a XAENOCS Xeuss 2.0 system X-ray scattering instrument at the University of Pennsylvania. The instrument was equipped with a GeniX3D Cu beam source with a wavelength of $\lambda = 1.54$ Å. Silver behenate was chosen as the standard material for calibration. All 2D scattering patterns were integrated into 1D plots of scattering intensity (I) versus q by the Foxtrot software. Elemental analysis was performed

by Galbraith Laboratories, Knoxville, TN. An LR Technologies Xtreme 206-11K Hot/Cold Plate was used to heat films during film fabrication. A BlakRay XX40BLB 40-watt (365-nm) UV lamp was used to cross-link thick, free-standing films of monomers **1a–f**. An adjustable micrometer film-casting doctor blade (50 mm standard width) was used for the preliminary TFC membrane solution-casting studies. A JEOL 7500F field-emission scanning electron microscope (HRSEM) at the University of Pennsylvania was used for fabricated TFC membrane characterization.

III.   Monomer Syntheses & Characterizations

3,4,5-Tris(11'-acryloyloxyundecyloxy)benzoic acid (2)[1]

This compound was synthesized as described in the literature.[1] Spectroscopic characterization and purity data for this compound matched published data.[1]
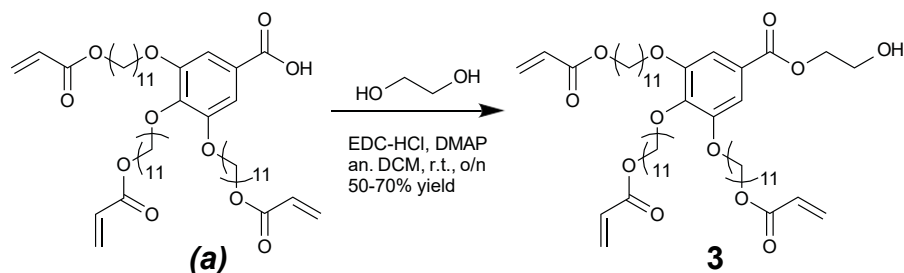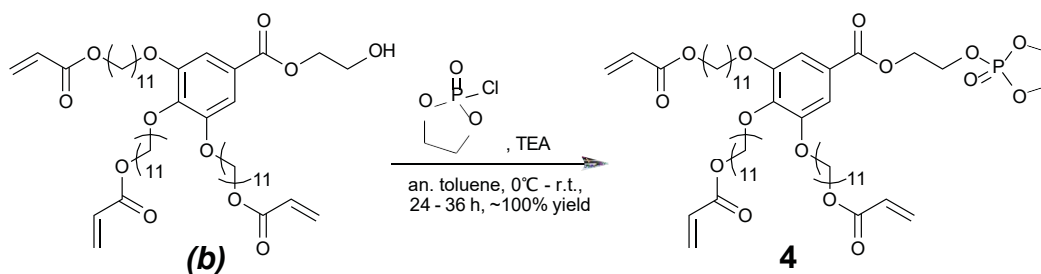

Scheme S1 Synthesis of compound **3** from 3,4,5-tris(11'-acryloyloxyundecyloxy)benzoic acid (**2**).

3,4,5-Tris-(11-acryloyloxy-undecyloxy)-benzoic acid 2-hydroxy-ethyl ester (3)

3,4,5-Tris(11'-acryloyloxyundecyloxy)benzoic acid (**2**) (10.0 g, 11.9 mmol), *N*-(3-dimethylaminopropyl)-*N′*-ethylcarbodiimide hydrochloride (EDC-HCl) (2.50 g, 13.0 mmol), and 4-dimethylaminopyridine (DMAP) (0.435 g, 3.56 mmol) were placed in a flame-dried, 250-mL Schlenk flask equipped with a stir bar, dissolved in anhydrous dichloromethane (DCM) (200 mL), and allowed to stir for 15–30 min at room temperature under light Ar flush. Anhydrous ethylene glycol (2.22 g, 35.8 mmol) was then added dropwise under light Ar flush and with vigorous stirring. The resulting solution was allowed to react for 18 h (i.e., overnight) at room temperature under static Ar. The following day, the organic solution was extracted with 0.5 M aq. HCl (3 x 100 mL), saturated aq. NaHCO₃ (3 x 100 mL), and saturated brine solution (3 x 100 mL). The organic phase was then dried over anhydrous sodium sulfate, filtered, and the solvent was removed via rotary evaporation. According to thin-layer chromatography (TLC) analysis of the resulting oil, the first spot (higher R_f) is unreacted starting material (**2**) and the second spot (lower R_f) is the hydroxy-ester target. The viscous yellow oil was then dissolved in a minimum amount of 1:1 (v/v) hexanes:ethyl acetate and loaded onto a wetted silica gel column (Chemglass 24/40, 1000-mL reservoir, 2.5" ID x 8" EL, course frit column). The column was eluted with 1 L of 1:1 hexanes:ethyl acetate solvent, and 20-mL fractions were

collected. Appropriate fractions, containing only the lower R_f spot, were combined and dried in vacuo to afford compound **3** as a white powder. Yield: 73%. ^{1}H NMR (300 MHz, DMSO-d_6): δ 7.20 (s, 2H), 6.27 (d, *J* = 17.2 Hz, 3H), 6.09 (ddd, *J* = 17.3, 10.2, 2.2 Hz, 3H), 5.85 (d, *J* = 10.1 Hz, 3H), 4.89 (t, *J* = 5.7 Hz, 1H), 4.22 (t, *J* = 5.0 Hz, 2H), 4.03 (t, *J* = 6.7 Hz, 6H), 3.90 (dt, *J* = 16.3, 6.2 Hz, 6H), 3.67 (q, *J* = 5.4 Hz, 2H), 1.70 – 1.51 (m, 12H), 1.44 – 1.36 (m, 6H), 1.24 (d, *J* = 12.0 Hz, 36H). ^{13}C NMR (75 MHz, DMSO-d_6): δ 165.25, 152.31, 130.81, 130.78, 128.32, 128.30, 107.45, 72.41, 68.43, 66.46, 63.93, 63.90, 59.06, 29.91, 29.27, 29.15, 29.07, 29.05, 28.91, 28.84, 28.80, 28.15, 25.66, 25.48, 25.45. FTIR (neat): 2930, 2855, 1718, 1636, 1588, 1498, 1465, 1431, 1409, 1334, 1275, 1200, 1115, 965, 891, 812, 723, 671. Elemental Analysis: Calcd for $C_{51}H_{82}O_{12}$: C, 69.04; H, 9.32; N, 0.00. Found: C, 69.19; H, 9.40; N, <0.50 (under detection limit).

Scheme S2 Synthesis of compound **4** from compound **3**.

3,4,5-Tris-(11-acryloyloxy-undecyloxy)-benzoic acid 2-(2-oxo-2λ⁵-[1,3,2]dioxaphospholan-2-yloxy)-ethyl ester (4)

Compound **3** (7.37 g, 8.31 mmol) and anhydrous triethylamine (TEA) (1.68 g, 16.6 mmol) were added to a flame-dried, 250-mL Schlenk flask equipped with a stir bar, dissolved in anhydrous toluene (150 mL), and allowed to stir for 15–30 min in an ice bath (0 °C) under light Ar flush. 2-Chloro-2-oxo-1,3,2-dioxaphospholane (CODP) (1.30 g, 9.14 mmol) was then added dropwise. The resulting solution was vigorously stirred at 0 °C for 15–30 min before removing the ice bath and allowing the solution to raise to room temperature under light Ar flush. The solution then reacted for 24–36 h at room temperature under static Ar. An ammonium salt by-product precipitated out as a white solid almost immediately. Later, the unwanted precipitate was filtered out via a Celite™ 545 plug and rinsed with cold (–25 °C) toluene. The solvent was then removed via rotary evaporation to afford compound **4** as a viscous, faintly yellow oil that was subsequently used without further purification. Yield: ~100%. ^{1}H NMR (300 MHz, methanol-d_4): δ 7.32 (s, 2H), 6.36 (dd, *J* = 17.4, 1.7 Hz, 3H), 6.13 (dd, *J* = 17.3, 10.3 Hz, 3H), 5.85 (dd, *J* = 10.5, 1.7 Hz, 3H), 4.58 – 4.35 (m, 4H), 4.11 (q, *J* = 6.0, 5.3 Hz, 8H), 4.00 (t, *J* = 6.2 Hz, 6H), 3.71 (q, *J* = 5.2, 4.7 Hz, 2H), 1.71 (ddt, *J* = 37.4, 13.6, 7.0 Hz, 12H), 1.51 (p, *J* = 6.9 Hz, 6H), 1.44 – 1.29 (m, 36H).

Note: Excess CODP, while necessary to promote full conversion, proved difficult to remove at this stage as the dioxaphospholane moiety of the intermediate is subject to cleavage upon use of harsh conditions. Therefore, the dioxaphospholane intermediate

was used without further purification and only ¹H NMR analysis was utilized to characterize the structure (shown in Fig. S1, below). Any impurities were removed upon purification of the final monomer products 1a–f made from compound 4.

¹H NMR (300 MHz, Methanol-d_4) δ 7.32 (s, 2H), 6.36 (dd, J = 17.4, 1.7 Hz, 3H), 6.13 (dd, J = 17.3, 10.3 Hz, 3H), 5.85 (dd, J = 10.5, 1.7 Hz, 3H), 4.58 – 4.35 (m, 4H), 4.11 (q, J = 6.0, 5.3 Hz, 8H), 4.00 (t, J = 6.2 Hz, 6H), 3.71 (q, J = 5.2, 4.7 Hz, 2H), 1.71 (ddt, J = 37.4, 13.6, 7.0 Hz, 12H), 1.51 (p, J = 6.9 Hz, 6H), 1.44 – 1.29 (m, 36H).
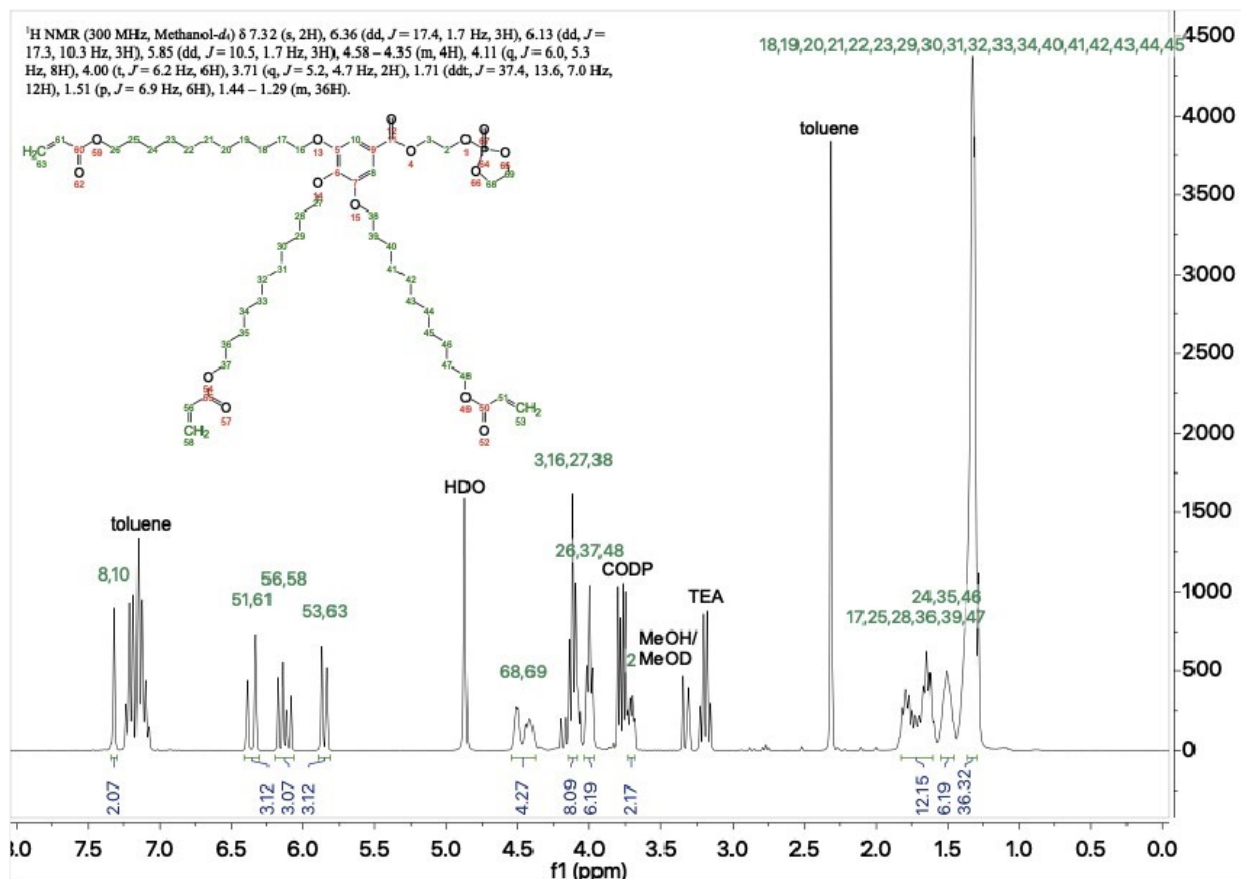
Fig. S1 ¹H NMR spectrum of the crude dioxaphospholane intermediate revealing several solvent impurities and excess CODP reagent. Deuterated solvent and other residual peaks are labeled in black (above peaks), hydrogen assignments are labeled in green (above peaks), and integration ranges are labeled in blue (below peaks).

Synthesis of monomers 1a–f from compound 4

Monomers **1a–f** were prepared from reaction of a tertiary amine with compound **4** as shown in Scheme S3. Detailed synthesis and structural characterization information for each of these new monomers are listed below. The newly synthesized derivatives are zwitterionic organic compounds that are difficult to dry completely and usually do not combust well. However, their obtained elemental analysis values are within the accepted ±0.4% tolerance range for C, H, and N to be considered pure when the presence of associated water molecules is accounted for.[2] To further verify the structures and purities of the new phosphobetaine-based zwitterionic derivatives, ¹H NMR and ¹H-¹H COSY (correlated spectroscopy) 2D-NMR spectra of the final monomers have also been included to show the lack of impurities other than associated water. COSY is a useful

method for determining which signals arise from neighboring protons, thus, proving covalent bonds are present.[3] Correlations appear when there is proton spin-spin coupling; and where there is no coupling, no correlation is expected to appear.[3] A COSY spectrum contains a diagonal and cross-peaks (i.e., signals that are not on the diagonal and correspond to other signals on the same horizontal and vertical projections).[3] The cross-peaks indicate couplings between two proton signals up to three, or occasionally four, bonds away (e.g., H–C–C–H).[3] The diagonal consists of the 1D spectrum with single peaks suppressed.[3]

1a: R, R', R" = –CH₃

1b: R, R' = -CH₃, R" = –CH₂CH₃

1c: R, R' = -CH₃, R" = –n-C₆H₁₃

1d:

1e:

1f:
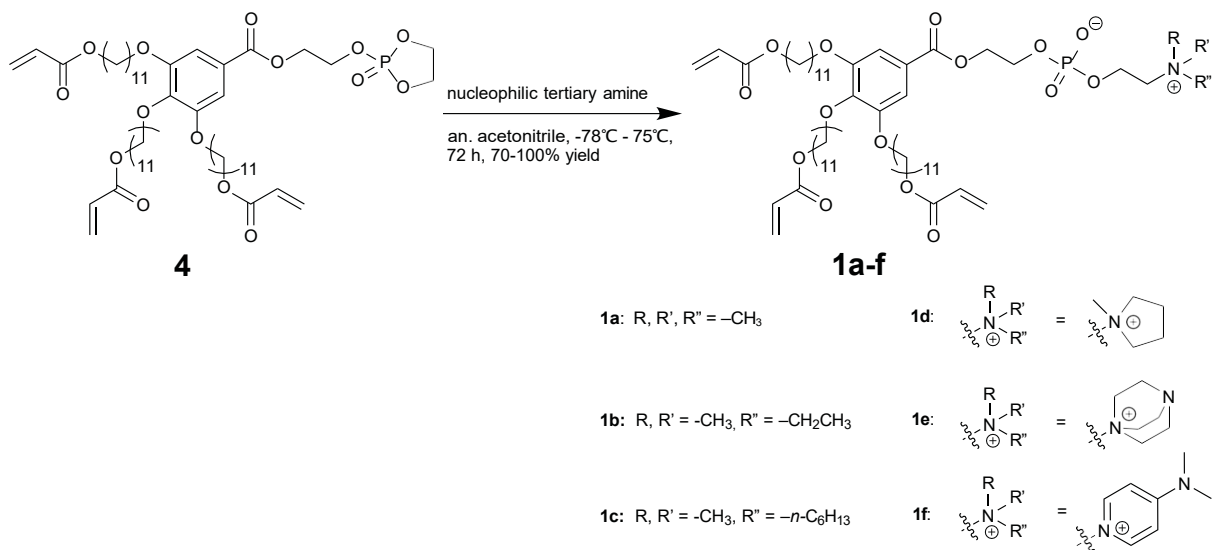
Scheme S3 Synthesis of monomers **1a–f** from compound **4**.

Monomer 1a

Compound **4** (1.38 g, 1.39 mmol) was dissolved in anhydrous acetonitrile (MeCN) (50 mL) and transferred via syringe to a pressure bottle equipped with a stir bar, a rubber septum, and an Ar needle inlet. The solution was then cooled to –78 °C in an acetone/dry ice bath (will cause solution to freeze). Trimethylamine (1 M solution in THF, AcroSeal™) (6.95 mL, 6.95 mmol) was added dropwise to the pressure vessel at –78 °C under light Ar flush. After about 5 min, the Ar needle inlet and rubber septum were removed and the pressure bottle was quickly sealed. The acetone/dry ice bath was then replaced with an oil bath and the vessel was heated to 75 °C. The solution was allowed to vigorously stir under pressure and heat for 72 h behind a polycarbonate safety shield. Later, the pressure bottle was cooled back to –78 °C and carefully opened. After warming to room temperature, the solvent was filtered through a Büchner funnel to separate any precipitate and was then removed via rotary evaporation. The oily product was redissolved in toluene and allowed to chill to –25 °C in the freezer. Again, the solvent was filtered of any precipitate via a Büchner funnel and was removed via rotary evaporation. The oily product was redissolved in a minimum amount of ethyl acetate and precipitated from a 2:1 (v/v) hexanes:ethyl acetate solution at –78 °C. The waxy product was dissolved in DCM (50 mL) and extracted with deionized (DI) water (3 x 50 mL) and saturated brine solution (3 x

50 mL). The organic phase was then dried over anhydrous sodium sulfate, filtered, and dried in vacuo to afford pure monomer **1a** as a beige, waxy solid. Yield: 89%. ^{1}H NMR (300 MHz, DMSO-d_6): δ 7.18 (s, 2H), 6.29 (dd, J = 17.2, 1.8 Hz, 3H), 6.12 (ddd, J = 17.2, 10.2, 1.8 Hz, 3H), 5.89 (dd, J = 10.2, 1.8 Hz, 3H), 4.39 – 4.29 (m, 2H), 4.05 (td, J = 6.6, 1.7 Hz, 8H), 3.91 (dt, J = 21.0, 6.2 Hz, 8H), 3.57 – 3.51 (m, 2H), 3.13 (s, 9H), 1.61 (dp, J = 27.9, 7.0, 6.6 Hz, 12H), 1.39 (d, J = 7.7 Hz, 6H), 1.26 (d, J = 12.9 Hz, 36H). ^{13}C NMR (75 MHz, DMSO-d_6): δ 165.40, 152.37, 131.16, 131.14, 128.36, 128.34, 107.38, 72.48, 68.47, 64.01, 63.98, 53.05, 29.87, 29.21, 29.11, 29.08, 29.03, 28.99, 28.89, 28.76, 28.74, 28.12, 25.67, 25.63, 25.43. FTIR (neat): 3403, 2922, 2851, 1730, 1584, 1465, 1431, 1372, 1334, 1215, 1163, 1107, 1074, 969, 869, 812, 794, 764, 723. Elemental Analysis: Calcd for $C_{56}H_{94}NO_{15}P$: C, 63.92; H, 9.00; N, 1.33. Calcd for $C_{56}H_{94}NO_{15}P \bullet 2H_2O$: C, 61.80; H, 9.08; N, 1.29. Found: C, 61.71; H, 8.98; N, 1.30.
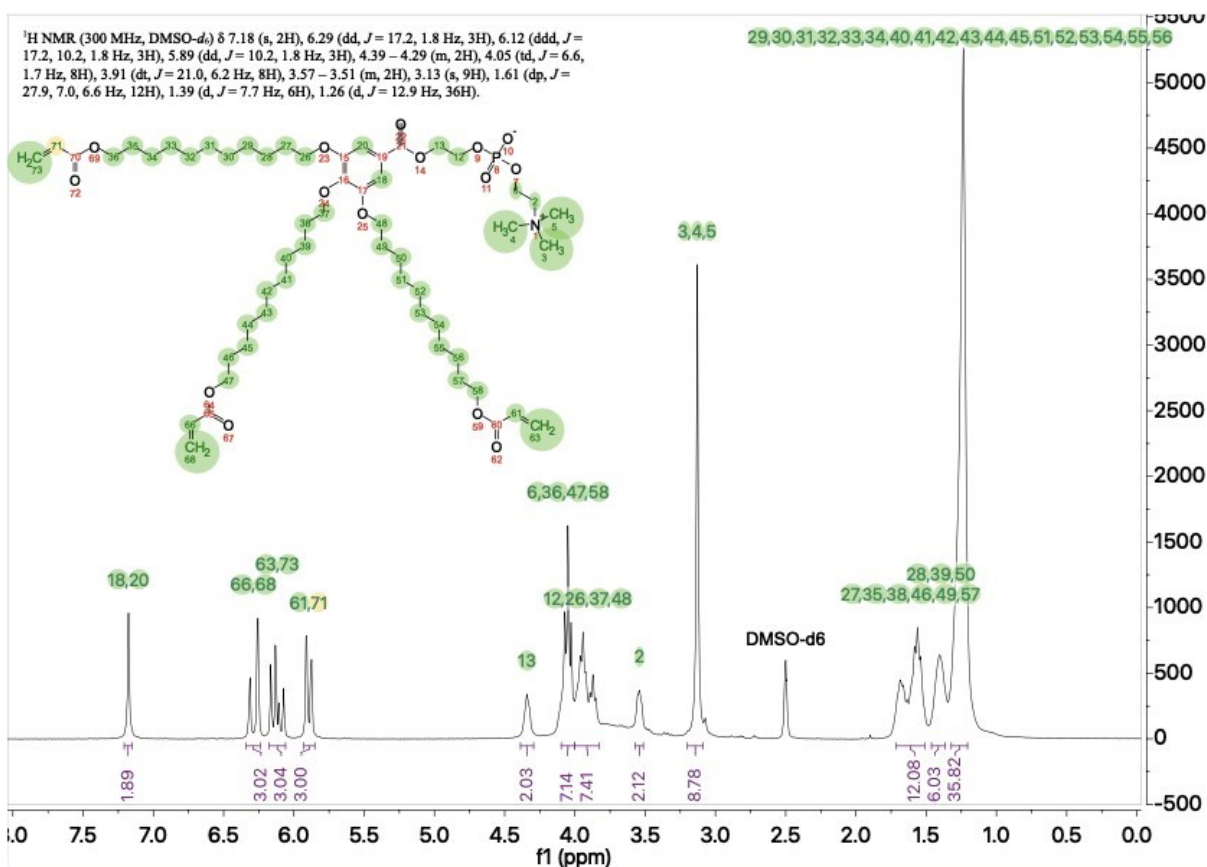

Fig. S2 ^{1}H NMR spectrum of monomer **1a** revealing only deuterated solvent peaks and no other impurities. Deuterated solvent residual peaks are labeled in black (above peaks), hydrogen assignments are labeled in green (above peaks), and integration ranges are labeled in purple (below peaks).
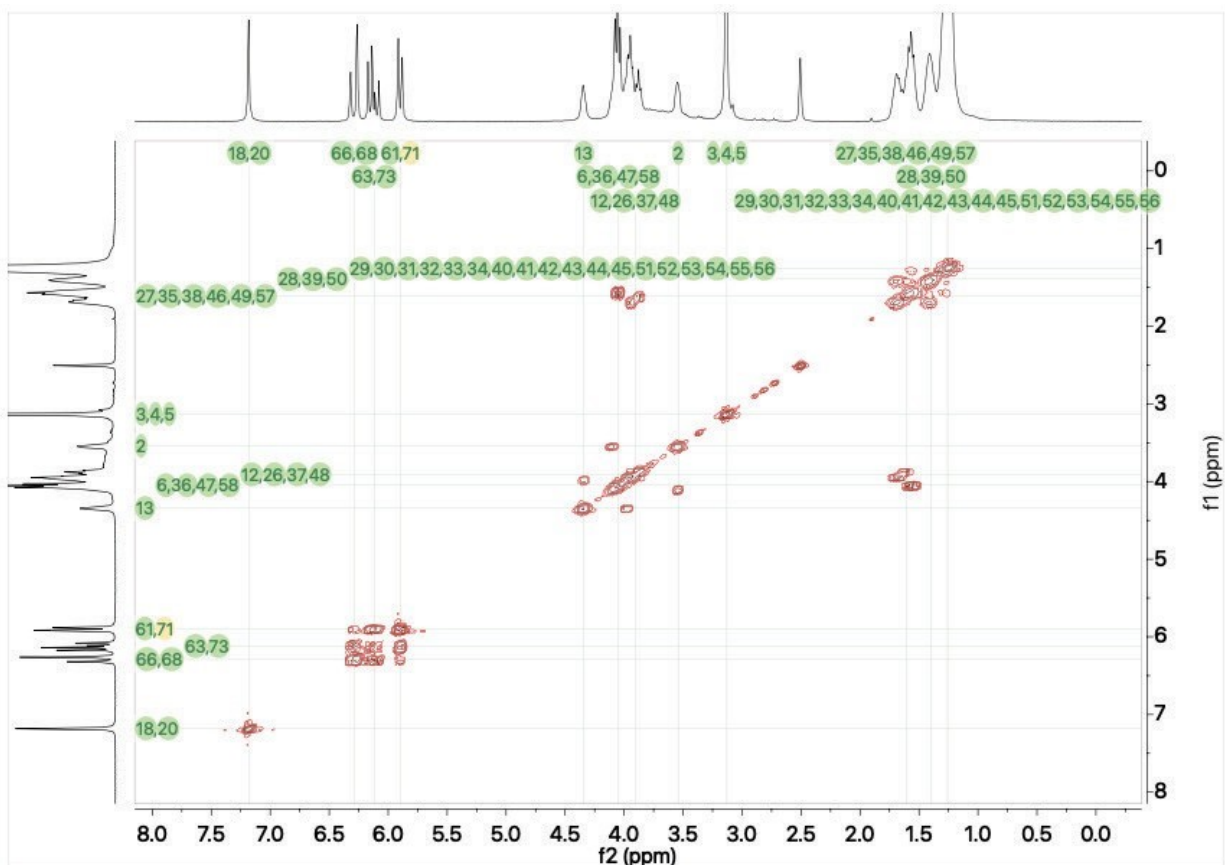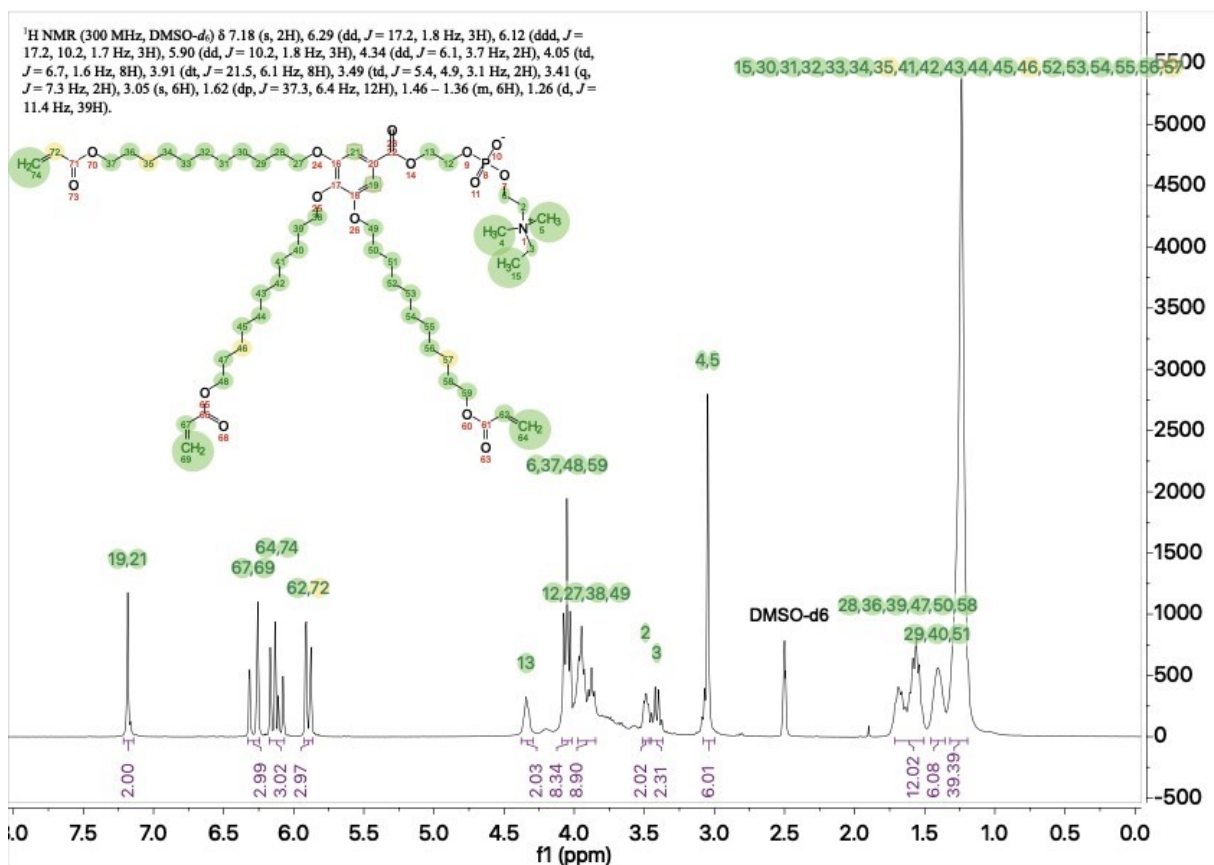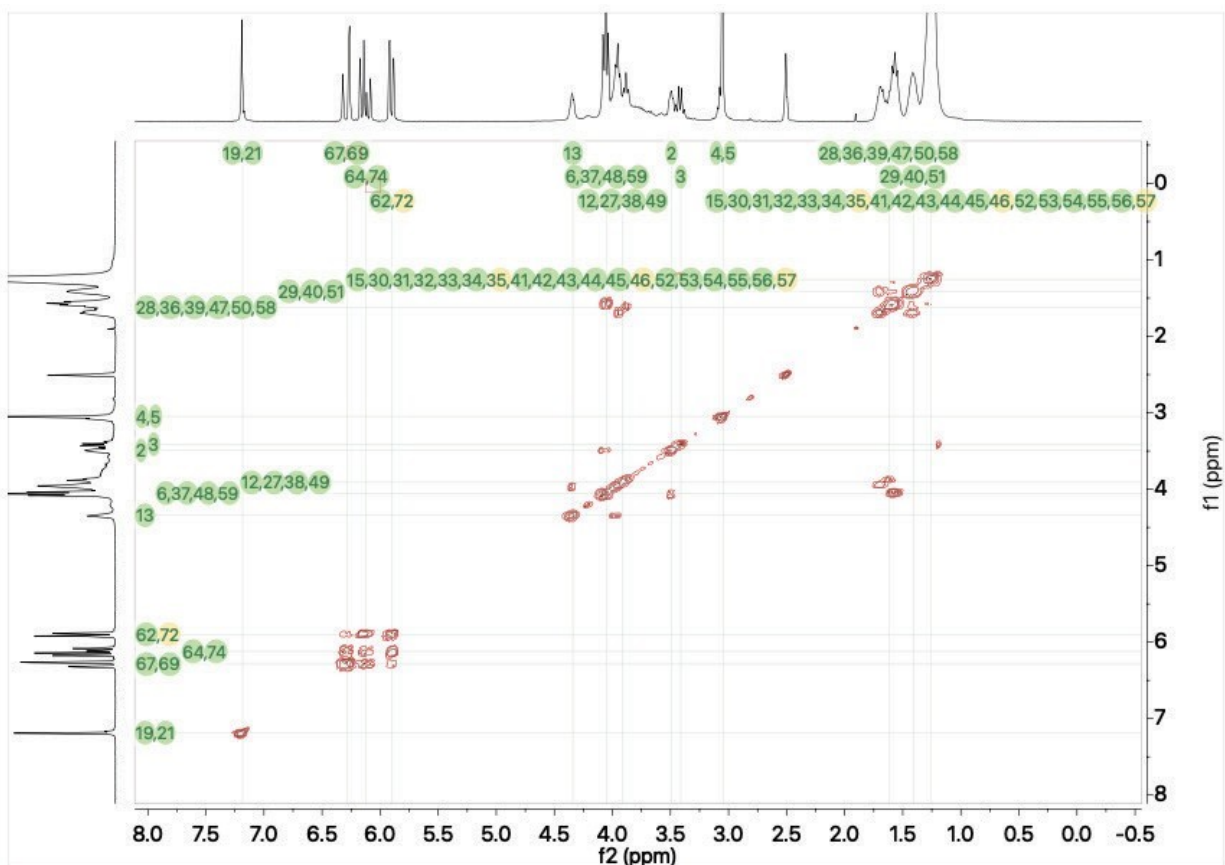
Fig. S3 ^{1}H-^{1}H COSY 2D-NMR spectrum of monomer **1a** revealing correlations within the zwitterionic headgroup. Hydrogen assignments are labeled in green.

Monomer 1b

Monomer **1b** was synthesized using the same procedure as that described for monomer **1a** except that *N,N*-dimethylethylamine (0.51 g, 6.95 mmol) was used instead of trimethylamine to react with compound **4** (1.38 g, 1.39 mmol). After the same workup procedure, pure **1b** was obtained as a yellow, waxy solid. Yield: 86%. ^{1}H NMR (300 MHz, DMSO-d_6): δ 7.18 (s, 2H), 6.29 (dd, J = 17.2, 1.8 Hz, 3H), 6.12 (ddd, J = 17.2, 10.2, 1.7 Hz, 3H), 5.90 (dd, J = 10.2, 1.8 Hz, 3H), 4.34 (dd, J = 6.1, 3.7 Hz, 2H), 4.05 (td, J = 6.7, 1.6 Hz, 8H), 3.91 (dt, J = 21.5, 6.1 Hz, 8H), 3.49 (td, J = 5.4, 4.9, 3.1 Hz, 2H), 3.41 (q, J = 7.3 Hz, 2H), 3.05 (s, 6H), 1.62 (dp, J = 37.3, 6.4 Hz, 12H), 1.46 – 1.36 (m, 6H), 1.26 (d, J = 11.4 Hz, 39H). ^{13}C NMR (75 MHz, DMSO-d_6): δ 165.43, 152.39, 131.20, 131.18, 128.36, 128.35, 107.39, 72.49, 68.49, 64.02, 62.51, 59.66, 50.16, 29.87, 29.21, 29.11, 29.08, 29.03, 28.99, 28.88, 28.76, 28.74, 28.13, 25.67, 25.63, 25.43, 7.86. FTIR (neat): 3381, 2922, 2851, 1730, 1584, 1495, 1461, 1431, 1372, 1334, 1215, 1163, 1074, 969, 861, 812, 764, 723. Elemental Analysis: Calcd for $C_{57}H_{96}NO_{15}P$: C, 64.20; H, 9.07; N, 1.31. Calcd for $C_{57}H_{96}NO_{15}P \bullet 3H_2O$: C, 61.11; H, 9.18; N, 1.25. Found: C, 61.16; H, 8.94; N, 1.31.

¹H NMR (300 MHz, DMSO-*d₆*) δ 7.18 (s, 2H), 6.29 (dd, *J* = 17.2, 1.8 Hz, 3H), 6.12 (ddd, *J* = 17.2, 10.2, 1.7 Hz, 3H), 5.90 (dd, *J* = 10.2, 1.8 Hz, 3H), 4.34 (dd, *J* = 6.1, 3.7 Hz, 2H), 4.05 (td, *J* = 6.7, 1.6 Hz, 8H), 3.91 (dt, *J* = 21.5, 6.1 Hz, 8H), 3.49 (td, *J* = 5.4, 4.9, 3.1 Hz, 2H), 3.41 (q, *J* = 7.3 Hz, 2H), 3.05 (s, 6H), 1.62 (dp, *J* = 37.3, 6.4 Hz, 12H), 1.46 – 1.36 (m, 6H), 1.26 (d, *J* = 11.4 Hz, 39H).
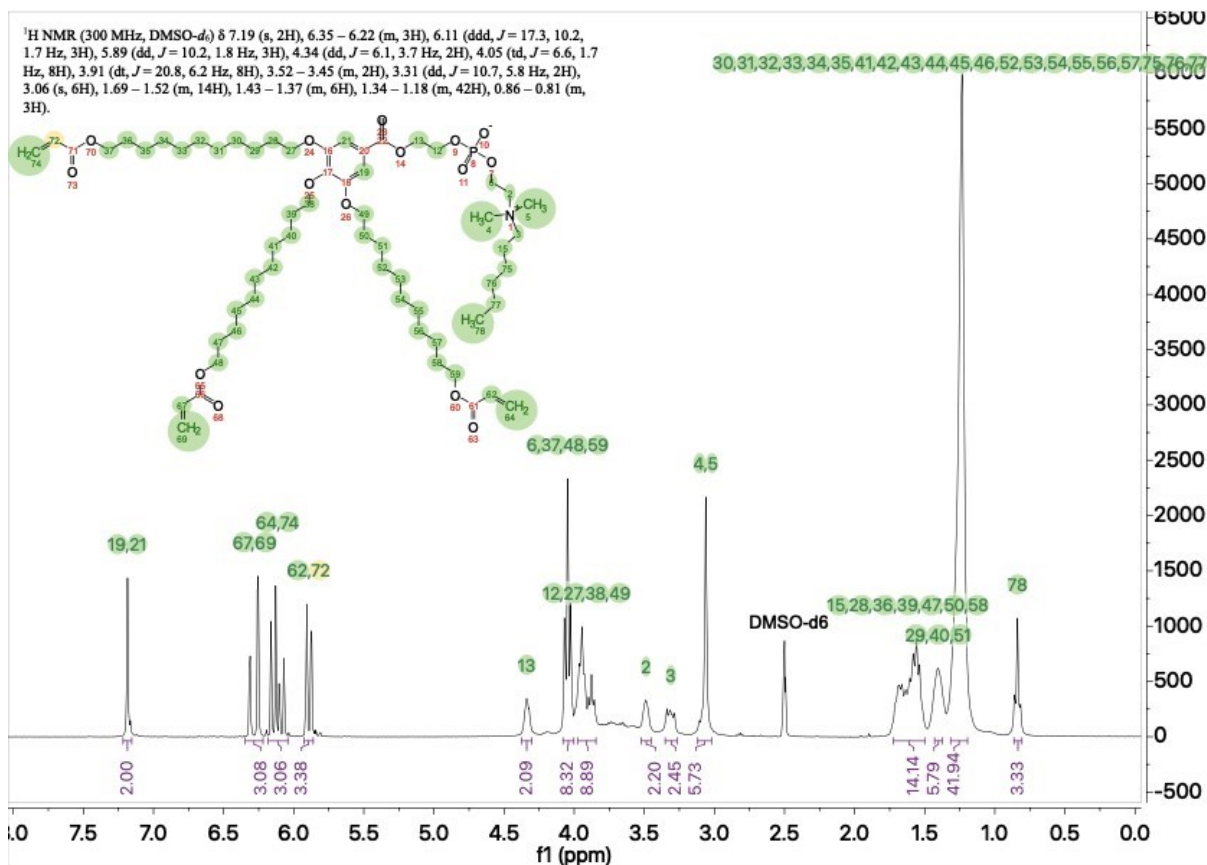
Fig. S4 ¹H NMR spectrum of monomer **1b** revealing only deuterated solvent peaks and no other impurities. Deuterated solvent residual peaks are labeled in black (above peaks), hydrogen assignments are labeled in green (above peaks), and integration ranges are labeled in purple (below peaks).

Fig. S5 ^{1}H-^{1}H COSY 2D-NMR spectrum of monomer **1b** revealing correlations within the zwitterionic headgroup. Hydrogen assignments are labeled in green.

Monomer 1c

Monomer **1c** was synthesized using the same procedure as that described for monomer **1a** except that *N,N*-dimethylhexylamine (0.90 g, 6.95 mmol) was used instead of trimethylamine to react with compound **4** (1.38 g, 1.39 mmol). After the same workup procedure, pure **1c** was obtained as a highly viscous, yellow wax. Yield: 88%. ^{1}H NMR (300 MHz, DMSO-d_6): δ 7.19 (s, 2H), 6.35 – 6.22 (m, 3H), 6.11 (ddd, *J* = 17.3, 10.2, 1.7 Hz, 3H), 5.89 (dd, *J* = 10.2, 1.8 Hz, 3H), 4.34 (dd, *J* = 6.1, 3.7 Hz, 2H), 4.05 (td, *J* = 6.6, 1.7 Hz, 8H), 3.91 (dt, *J* = 20.8, 6.2 Hz, 8H), 3.52 – 3.45 (m, 2H), 3.31 (dd, *J* = 10.7, 5.8 Hz, 2H), 3.06 (s, 6H), 1.69 – 1.52 (m, 14H), 1.43 – 1.37 (m, 6H), 1.34 – 1.18 (m, 42H), 0.86 – 0.81 (m, 3H). ^{13}C NMR (75 MHz, DMSO-d_6): δ 165.39, 152.38, 131.15, 131.13, 128.35, 128.33, 107.40, 72.48, 68.49, 64.12, 64.00, 63.98, 50.68, 30.72, 29.87, 29.21, 29.11, 29.08, 29.03, 28.99, 28.89, 28.74, 28.13, 25.67, 25.62, 25.43, 21.92, 21.74, 13.79. FTIR (neat): 3403, 2922, 2855, 1730, 1584, 1465, 1431, 1372, 1334, 1215, 1163, 1070, 965, 861, 812, 764, 723. Elemental Analysis: Calcd for $C_{61}H_{104}NO_{15}P$: C, 65.27; H, 9.34; N, 1.25. Calcd for $C_{61}H_{104}NO_{15}P \bullet 2.5H_2O$: C, 62.76; H, 9.41; N, 1.20. Found: C, 62.74; H, 9.02; N, 1.18.

Fig. S6 ^{1}H NMR spectrum of monomer **1c** revealing only deuterated solvent peaks and no other impurities. Deuterated solvent residual peaks are labeled in black (above peaks), hydrogen assignments are labeled in green (above peaks), and integration ranges are labeled in purple (below peaks).
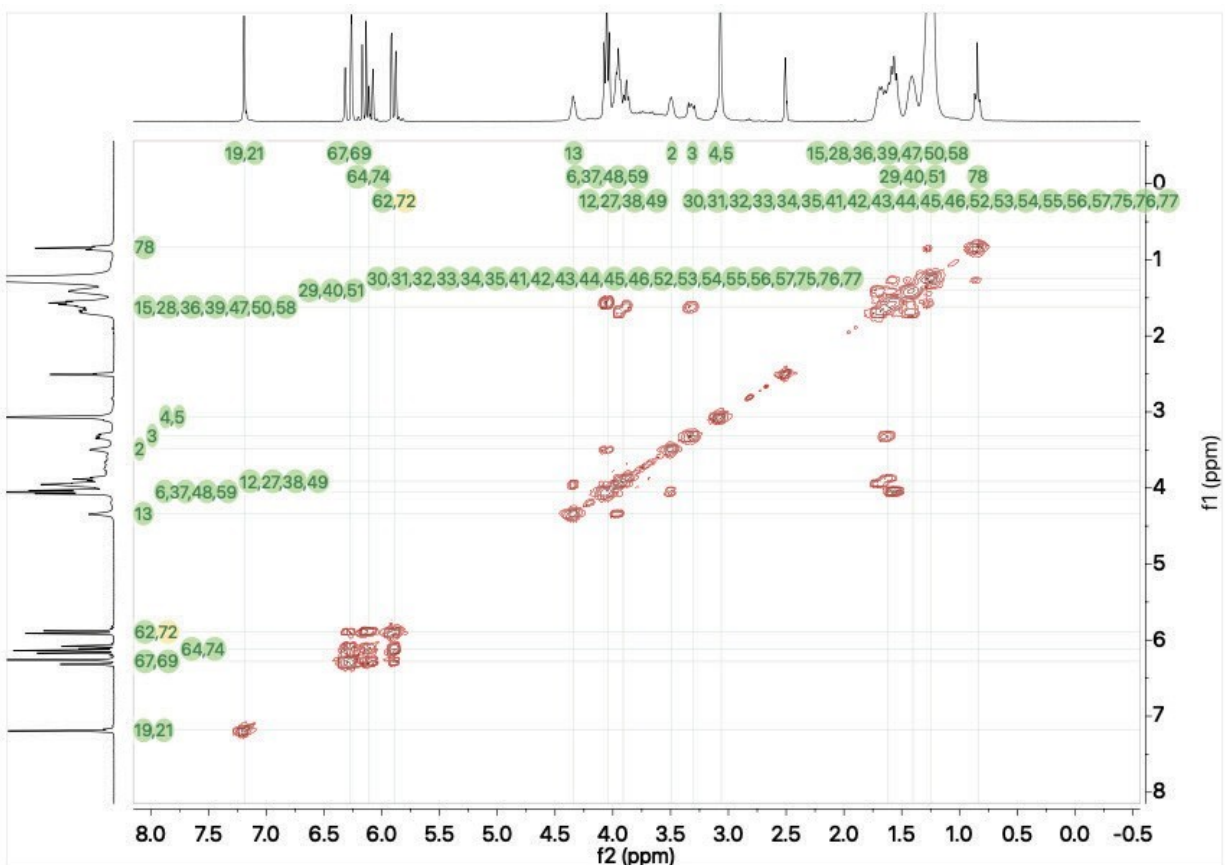
Fig. S7 ^{1}H-^{1}H COSY 2D-NMR spectrum of monomer **1c** revealing correlations within the zwitterionic headgroup. Hydrogen assignments are labeled in green.

Monomer 1d

Monomer **1d** was synthesized using the same procedure as that described for monomer **1a** except that 1-methylpyrrolidine (0.59 g, 6.95 mmol) was used instead of trimethylamine to react with compound **4** (1.38 g, 1.39 mmol). After the same workup procedure, pure **1d** was obtained as a beige, waxy solid. Yield: 81%. ^{1}H NMR (300 MHz, DMSO-d_6): δ 7.20 (s, 2H), 6.30 (dd, J = 17.3, 1.8 Hz, 3H), 6.14 (ddd, J = 17.3, 10.2, 1.3 Hz, 3H), 5.91 (dd, J = 10.2, 1.8 Hz, 3H), 4.34 (dd, J = 6.1, 3.7 Hz, 2H), 4.07 (td, J = 6.6, 1.1 Hz, 8H), 3.93 (dt, J = 22.1, 6.1 Hz, 8H), 3.56 – 3.50 (m, 6H), 3.05 (s, 3H), 2.09 – 2.01 (m, 4H), 1.63 (dp, J = 34.6, 6.6 Hz, 12H), 1.43 (d, J = 10.2 Hz, 6H), 1.25 (s, 36H). ^{13}C NMR (75 MHz, DMSO-d_6): δ 165.47, 152.40, 131.27, 128.38, 107.40, 72.52, 68.49, 64.23, 64.04, 47.61, 29.83, 29.16, 29.07, 29.03, 28.99, 28.94, 28.83, 28.70, 28.11, 25.64, 25.58, 25.40, 20.81. FTIR (neat): 3414, 2922, 2851, 1730, 1584, 1498, 1465, 1431, 1372, 1331, 1215, 1163, 1107, 1070, 951, 865, 812, 764, 723. Elemental Analysis: Calcd for $C_{58}H_{96}NO_{15}P$: C, 64.60; H, 8.97; N, 1.30. Calcd for $C_{58}H_{96}NO_{15}P \bullet 2H_2O$: C, 62.51; H, 9.05; N, 1.26. Found: C, 62.17; H, 9.06; N, 1.25.
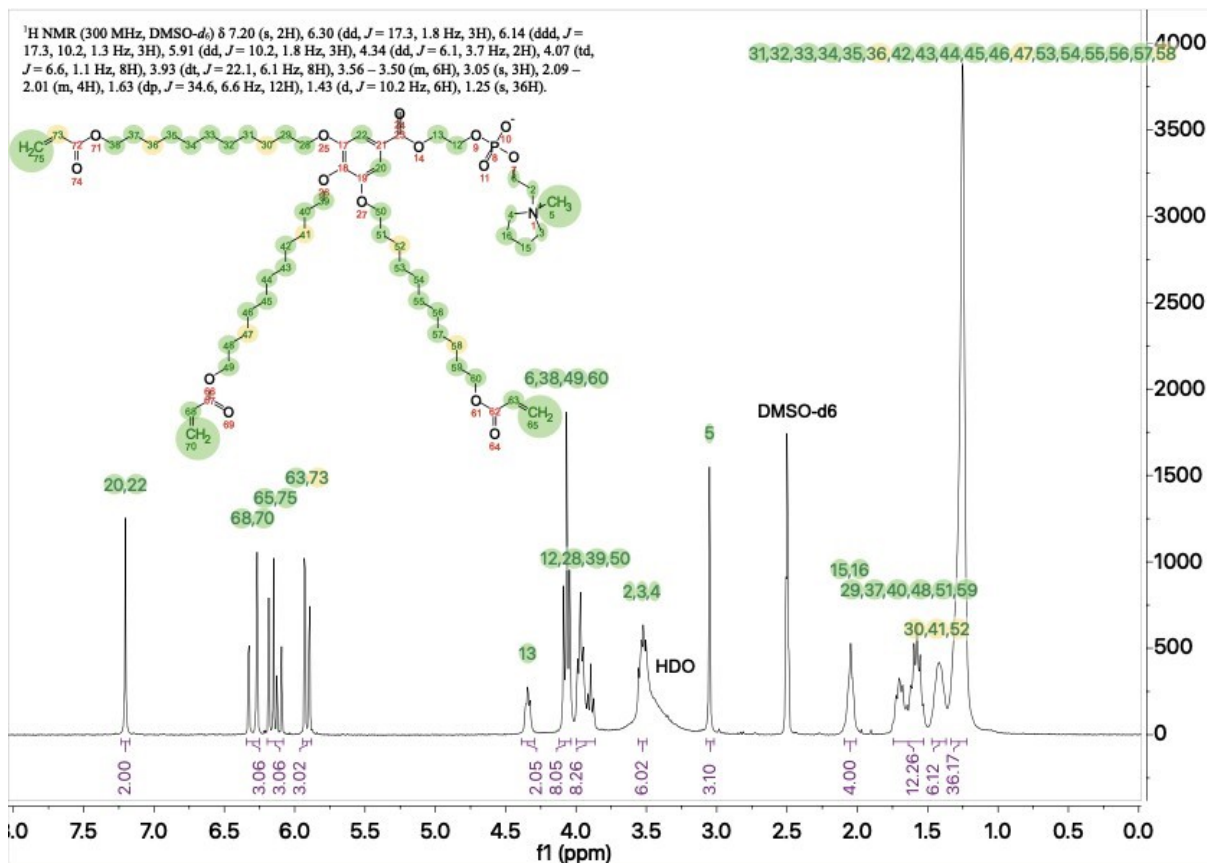
Fig. S8 ^{1}H NMR spectrum of monomer **1d** revealing only deuterated solvent peaks and no other impurities. Deuterated solvent residual peaks are labeled in black (above peaks), hydrogen assignments are labeled in green (above peaks), and integration ranges are labeled in purple (below peaks).
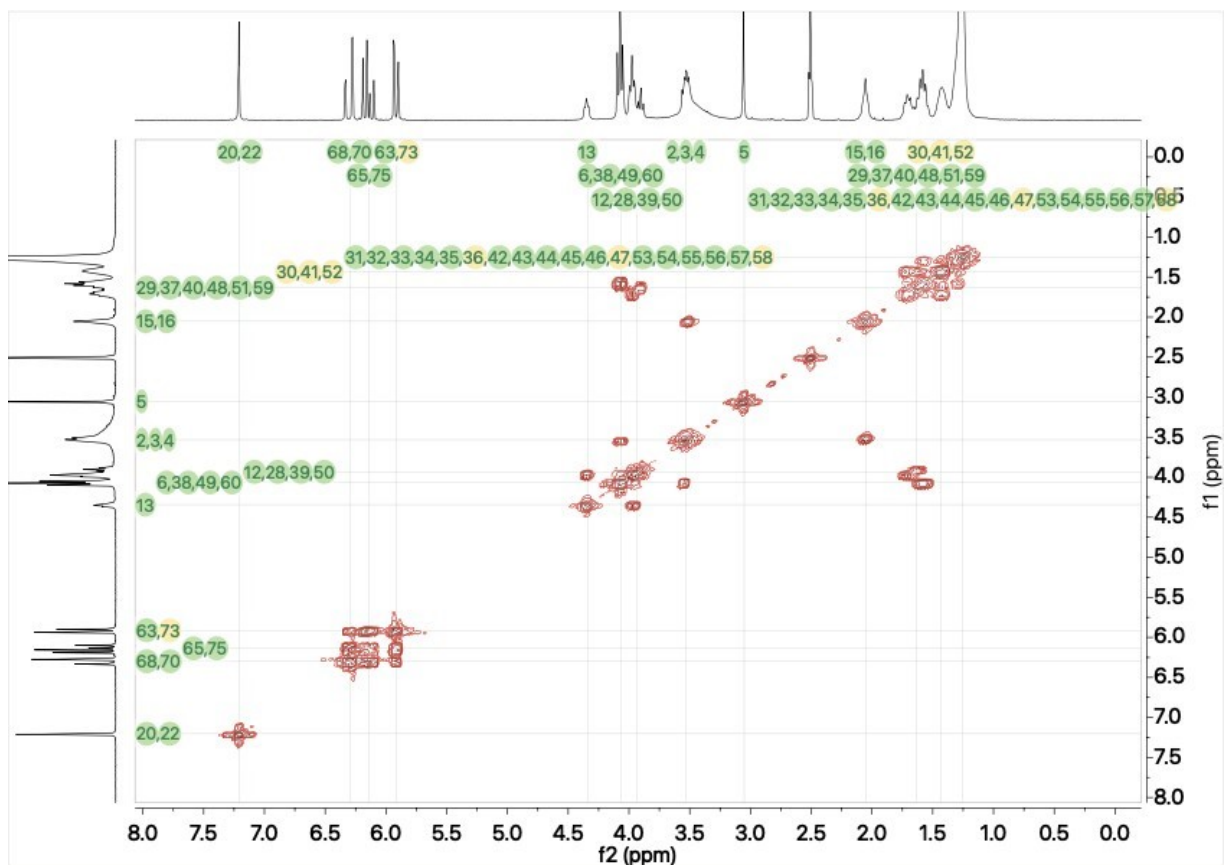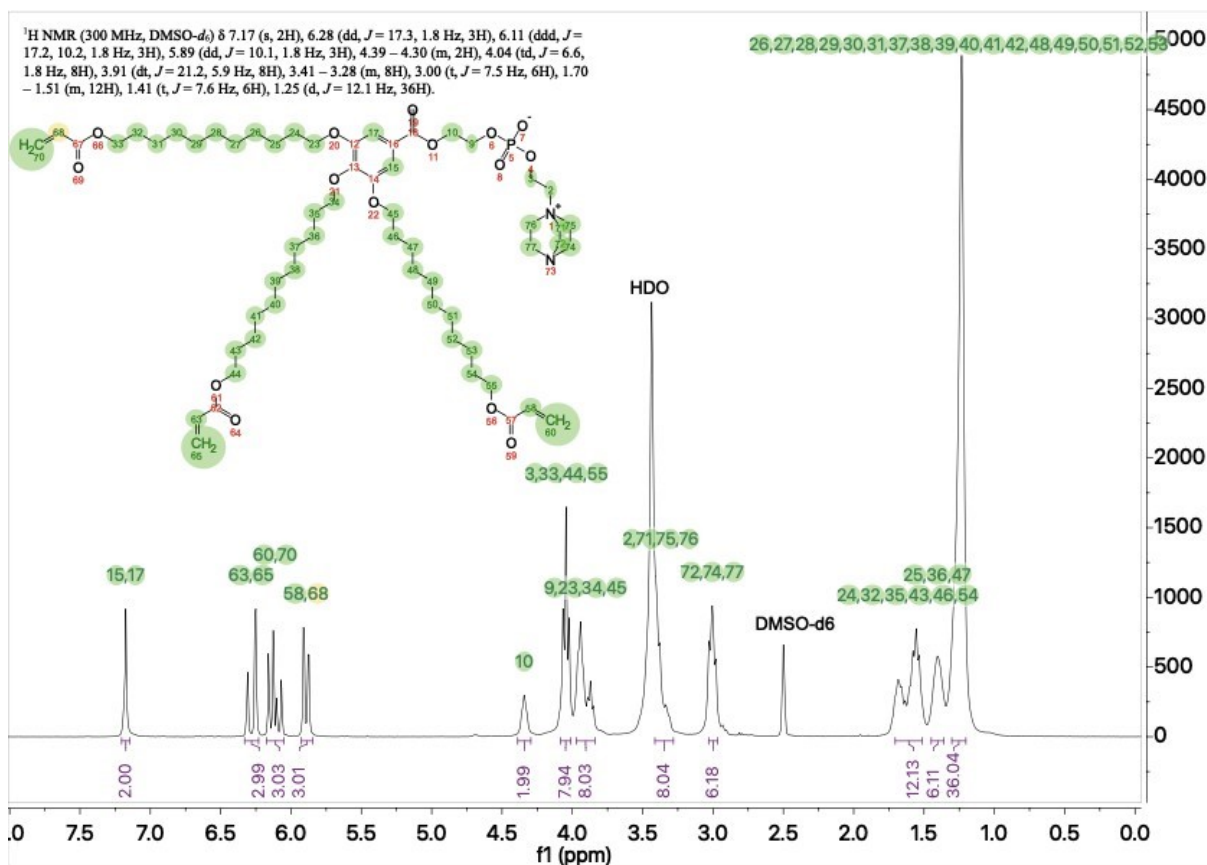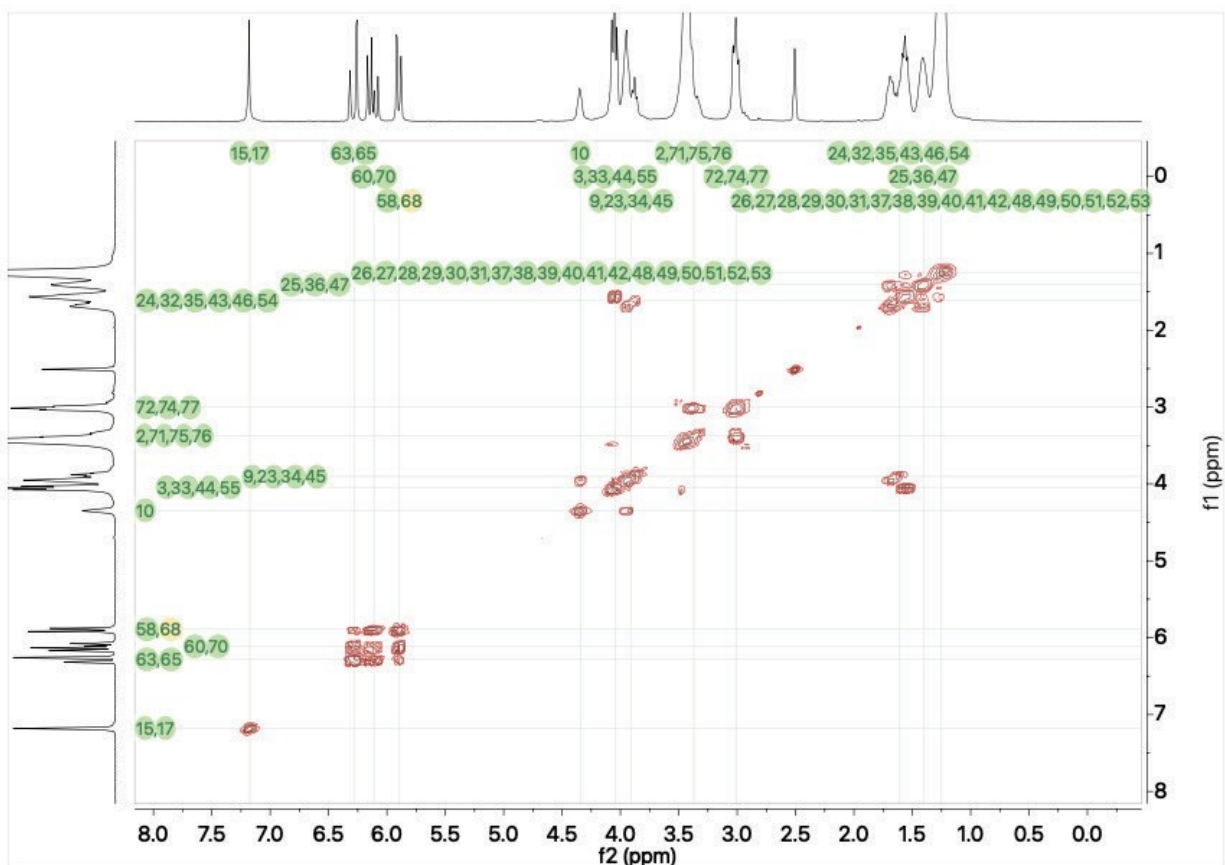
Fig. S9 ^{1}H-^{1}H COSY 2D-NMR spectrum of monomer **1d** revealing correlations within the zwitterionic headgroup. Hydrogen assignments are labeled in green.

Monomer 1e

Monomer **1e** was synthesized using the same procedure as that described for monomer **1a** except that 1,4-diazabicyclo[2.2.2]octane (DABCO) (0.78 g, 6.95 mmol) was used instead of trimethylamine to react with compound **4** (1.38 g, 1.39 mmol). After the same workup procedure, pure **1e** was obtained as a rosy beige, waxy solid. Yield: 76%. ^{1}H NMR (300 MHz, DMSO-d_6): δ 7.17 (s, 2H), 6.28 (dd, J = 17.3, 1.8 Hz, 3H), 6.11 (ddd, J = 17.2, 10.2, 1.8 Hz, 3H), 5.89 (dd, J = 10.1, 1.8 Hz, 3H), 4.39 – 4.30 (m, 2H), 4.04 (td, J = 6.6, 1.8 Hz, 8H), 3.91 (dt, J = 21.2, 5.9 Hz, 8H), 3.41 – 3.28 (m, 8H), 3.00 (t, J = 7.5 Hz, 6H), 1.70 – 1.51 (m, 12H), 1.41 (t, J = 7.6 Hz, 6H), 1.25 (d, J = 12.1 Hz, 36H). ^{13}C NMR (75 MHz, DMSO-d_6): δ 165.46, 152.40, 131.21, 131.19, 128.37, 128.35, 107.40, 72.51, 68.51, 64.03, 64.00, 52.33, 44.71, 29.89, 29.22, 29.13, 29.09, 29.04, 29.00, 28.90, 28.78, 28.75, 28.14, 25.69, 25.64, 25.44. FTIR (neat): 3392, 2922, 2851, 1730, 1584, 1498, 1465, 1372, 1334, 1215, 1163, 1103, 1074, 999, 958, 898, 842, 812, 790, 764, 723, 671. Elemental Analysis: Calcd for $C_{59}H_{97}N_2O_{15}P$: C, 64.11; H, 8.85; N, 2.53. Calcd for $C_{59}H_{97}N_2O_{15}P \bullet 3.25H_2O$: C, 60.88; H, 8.96; N, 2.41. Found: C, 60.61; H, 8.73; N, 2.81.

1H NMR (300 MHz, DMSO-d6) δ 7.17 (s, 2H), 6.28 (dd, J = 17.3, 1.8 Hz, 3H), 6.11 (ddd, J = 17.2, 10.2, 1.8 Hz, 3H), 5.89 (dd, J = 10.1, 1.8 Hz, 3H), 4.39 – 4.30 (m, 2H), 4.04 (td, J = 6.6, 1.8 Hz, 8H), 3.91 (dt, J = 21.2, 5.9 Hz, 8H), 3.41 – 3.28 (m, 8H), 3.00 (t, J = 7.5 Hz, 6H), 1.70 – 1.51 (m, 12H), 1.41 (t, J = 7.6 Hz, 6H), 1.25 (d, J = 12.1 Hz, 36H).

Fig. S10 1H NMR spectrum of monomer **1e** revealing only deuterated solvent peaks and no other impurities. Deuterated solvent residual peaks are labeled in black (above peaks), hydrogen assignments are labeled in green (above peaks), and integration ranges are labeled in purple (below peaks).

Fig. S11 ^{1}H-^{1}H COSY 2D-NMR spectrum of monomer **1e** revealing correlations within the zwitterionic headgroup. Hydrogen assignments are labeled in green.

Monomer 1f

Monomer **1f** was synthesized using the same procedure as that described for monomer **1a** except that 4-dimethylaminopyridine (DMAP) (0.85 g, 6.95 mmol) was used instead of trimethylamine to react with compound **4** (1.38 g, 1.39 mmol). After the same workup procedure, pure **1f** was obtained as a beige, waxy solid. Yield: 72%. ^{1}H NMR (300 MHz, DMSO-d_6): δ 8.31 (t, J = 8.7 Hz, 2H), 7.14 (s, 2H), 6.98 (d, J = 7.6 Hz, 2H), 6.27 (d, J = 17.2 Hz, 3H), 6.10 (dd, J = 17.2, 10.1 Hz, 3H), 5.88 (d, J = 10.2 Hz, 3H), 4.35 (d, J = 5.4 Hz, 2H), 4.26 (s, 2H), 4.04 (t, J = 6.6 Hz, 8H), 3.93 – 3.83 (m, 8H), 3.13 (s, 6H), 1.69 – 1.51 (m, 12H), 1.40 (t, J = 8.1 Hz, 6H), 1.25 (d, J = 15.5 Hz, 36H). ^{13}C NMR (75 MHz, DMSO-d_6): δ 165.39, 155.88, 152.35, 142.59, 131.11, 128.34, 128.31, 107.32, 72.47, 68.45, 63.99, 63.97, 62.24, 57.29, 39.62, 29.91, 29.25, 29.15, 29.11, 29.06, 29.03, 28.92, 28.80, 28.77, 28.14, 25.69, 25.45. FTIR (neat): 3392, 2922, 2851, 1730, 1651, 1573, 1498, 1431, 1331, 1211, 1167, 1107, 1059, 977, 939, 828, 812, 764, 719. Elemental Analysis: Calcd for $C_{60}H_{95}N_2O_{15}P$: C, 64.61; H, 8.59; N, 2.51. Calcd for $C_{60}H_{95}N_2O_{15}P$ • 1.5H_2O: C, 63.08; H, 8.65; N, 2.45. Found: C, 62.83; H, 8.51; N, 2.84.
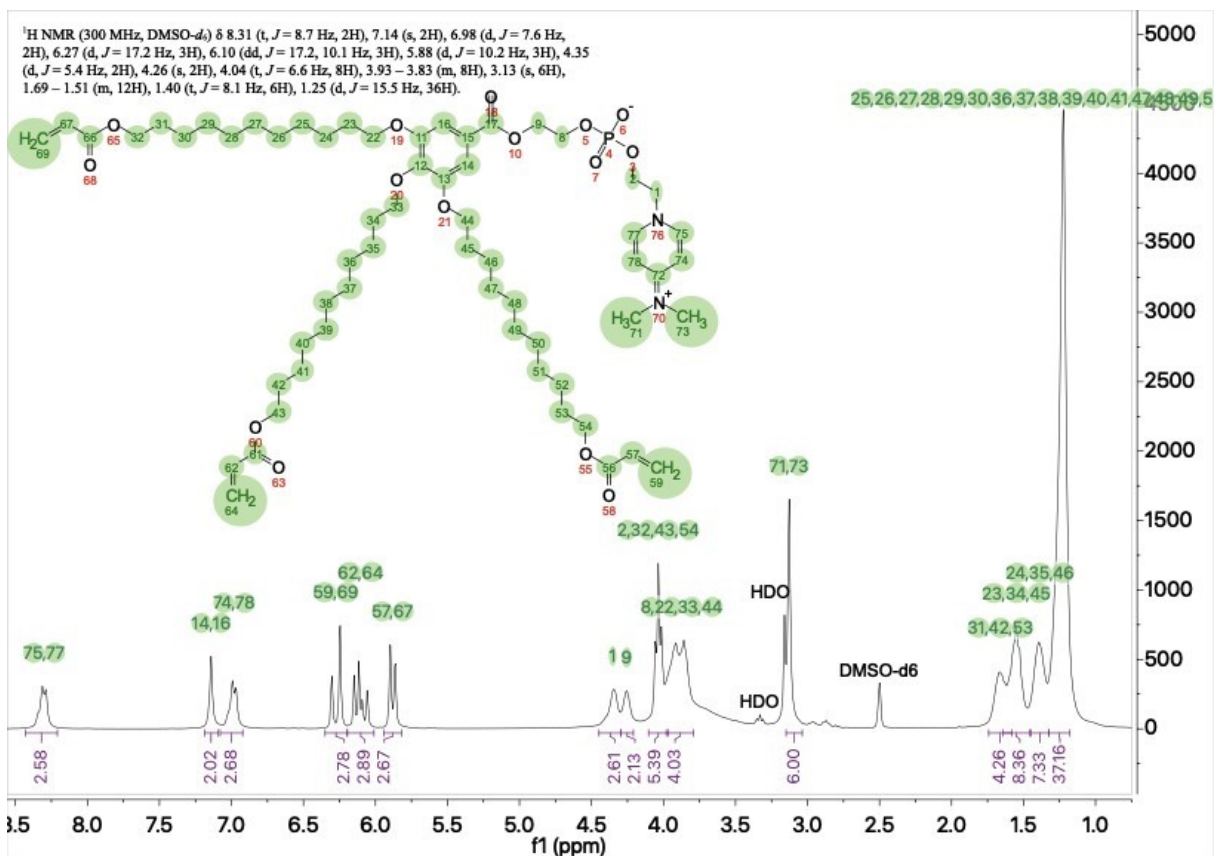
Fig. S12 ^{1}H NMR spectrum of monomer **1f** revealing only deuterated solvent peaks and no other impurities. Deuterated solvent residual peaks are labeled in black (above peaks), hydrogen assignments are labeled in green (above peaks), and integration ranges are labeled in purple (below peaks).
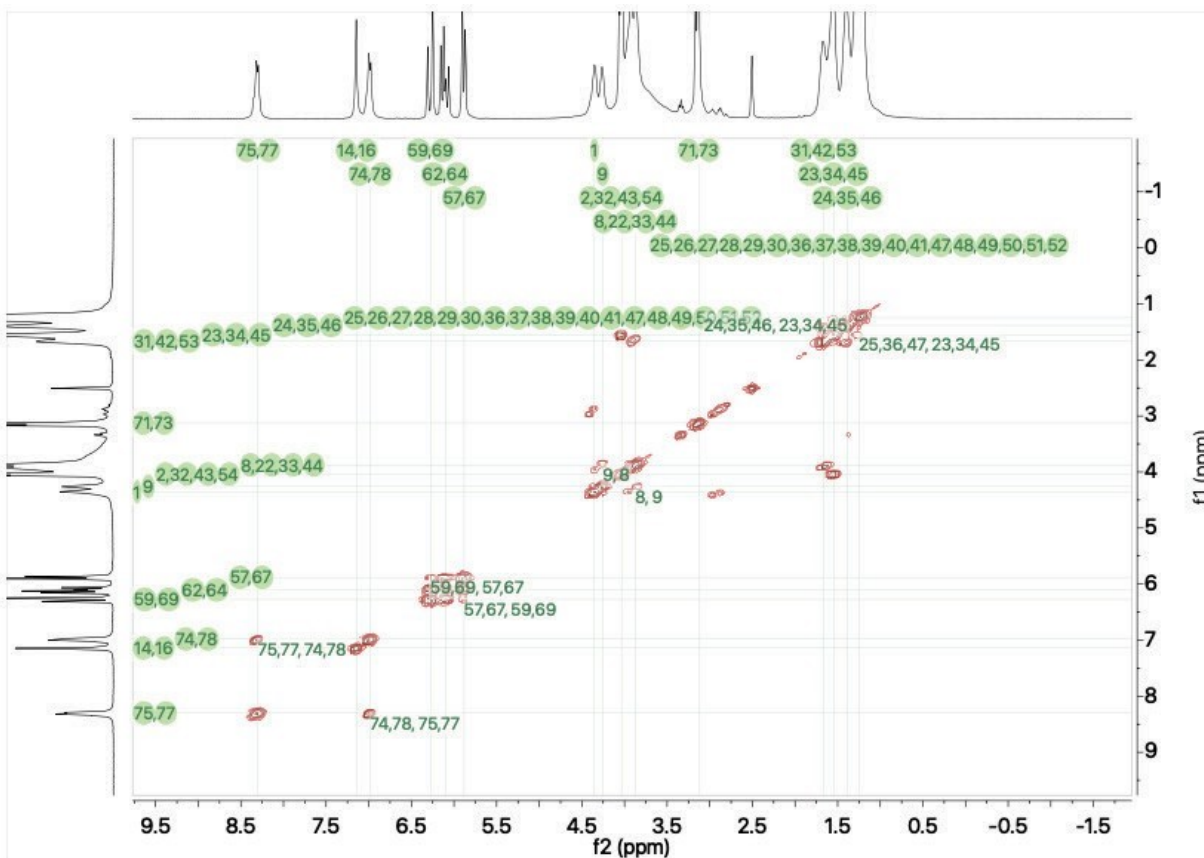
Fig. S13 ^{1}H-^{1}H COSY 2D-NMR spectrum of monomer **1f** revealing correlations within the zwitterionic headgroup. Hydrogen assignments are labeled in green.

*Note: An alternate convergent synthesis approach to monomers **1a–f** was also initially attempted by synthesizing the phosphobetaine headgroup units separately and then coupling them to 3,4,5-tris(11'-acryloyloxyundecyloxy)benzoic acid. However, this approach failed due to solubility issues: It was not possible to find a reaction solvent system that would mutually dissolve the highly polar phosphobetaine units and the relatively less-polar, benzoic acid wedge compound.*

IV.   Qualitative, PLM-based Solvent-Penetration Scan Screening of LLC Phase Behaviour

To determine the potential LLC phase behaviour of monomers **1a–f** (see Table S1) quickly and qualitatively with an added solvent, the PLM-based solvent-penetration scan technique was employed. This technique is a solvent-amphiphile gradient assay that quickly (i.e., in minutes) determines qualitatively (via PLM optical texture) what phases can be formed by the solvent-amphiphile pair throughout a specific temperature range.[2] This technique was performed by placing a pure monomer sample between a glass

microscope slide and a coverslip and pressing gently. The sandwiched sample was then placed on the PLM thermal stage and annealed to 100 °C. The sample was then slowly cooled back down to room temperature (22 ± 1 °C). A small amount (i.e., drop(s), <0.1 mL) of the chosen solvent was added to the edge of the cover slip and the solvent was drawn via capillary action into contact with the monomer, creating a concentration gradient. The specimen was then heated to 100 °C at a rate of 5 °C/min on the PLM thermal stage and its optical texture (under crossed polarizers as a function of temperature) was recorded via digital image capture (see Fig. S14). The differences in optical texture were used to determine the potential LLC phases formed. Since Q phases are black (i.e., isotropic) under PLM and are typically found between birefringent lamellar (L) and hexagonal (H) phases, a dark isotropic band between two birefringent regions indicates a potential Q phase.[2] The six new phosphobetaine-based monomers **1a–f** were evaluated in this fashion with added 0.1 M aq. NH$_4$Cl solution as the blending solvent. These results do not guarantee the presence of a Q phase without more detailed phase diagram analysis of carefully prepared mixtures via full PLM LLC-phase elucidation supported by PXRD and SAXS confirmation.

Note: It was found that LLC phases could also be induced via introduction of 0.1 M aq. LiCl solution or ethylammonium nitrate (EAN) ionic liquid. Unfortunately, the use of 0.1 M aq. LiCl solution did not result in the formation of any Q phases via PLM-based solvent-penetration scan screening. The Q-phase behaviour and characterization of this series of phosphobetaine monomers with EAN are part of ongoing research that will be reported in a separate future publication.

Table S1 Summary of the preliminary qualitative Q-phase formation behaviour of monomers **1a–f** studied in this work when mixed with 0.1 M aq. NH$_4$Cl and observed from 25–100 °C, as determined via PLM-based solvent-penetration scan screening studies.

1a: R, R', R'' = –CH$_3$
1b: R, R' = -CH$_3$, R'' = –CH$_2$CH$_3$
1c: R, R' = -CH$_3$, R'' = –n-C$_6$H$_{13}$
1d:
1e:
1f:
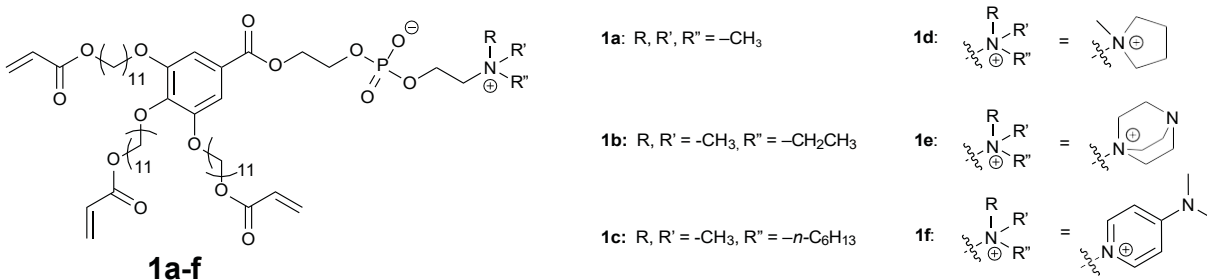
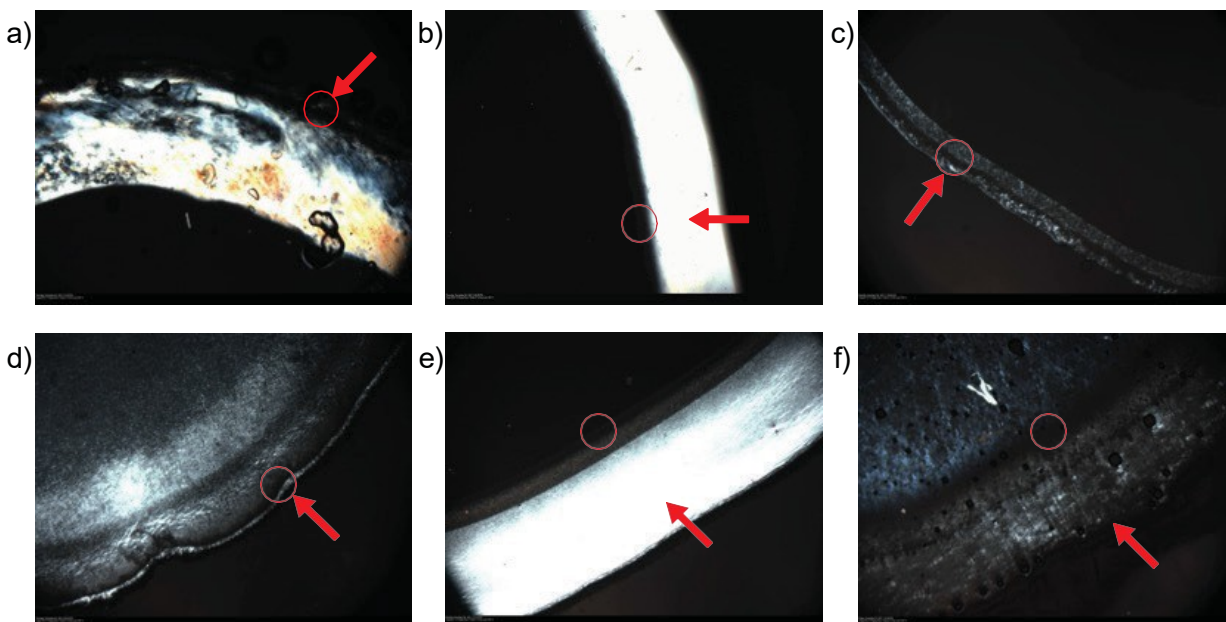| Monomer:	1a	1b	1c	1d	1e	1f
Potential Q Phase via Penetration Scan Studies:	Yes	Yes	Yes	Yes	Yes	Yes
Potential Q-phase Temp. Range (°C):	59.5–79.5	55.8–75.8	36.5–91.5	64.9–84.9	52.1–72.1	36.3–76.3

Fig. S14 Representative PLM images (magnification: 50x) of 0.1 M aq. NH_4Cl penetration scans of monomers **1a–f**: a) potential Q-phase formation for **1a** at 69.5 °C; b) potential Q-phase formation for **1b** at 65.8 °C; c) potential Q-phase formation in **1c** at 51.5 °C; d) potential Q-phase formation for **1d** at 74.9 °C, e) potential Q phase formation for **1e** at 62.1 °C; f) potential Q-phase formation in **1f** at 56.3 °C. The black (pseudo-isotropic) region between two bright, anisotropic LLC regions is indicative of the presence of a potential Q phase.[2] The arrows in the PLM images point in the direction of solvent penetration (i.e., decreasing solvent concentration) into the bulk material, and the circles emphasize the location of the optically black band.

V.   Full Phase Diagram Elucidation using PLM, PXRD, and SAXS Analyses

(a) Initial determination of different phase regions via variable-temperature PLM

LLC samples of specific composition were prepared by adding the desired mass of each monomer (i.e., **1a–f**) to tared glass vials placed on a microbalance, followed by the addition of an appropriate mass of 0.1 M aq. NH_4Cl solution via pipette. The vials were sealed with their corresponding cap and centrifuged at 4000 rpm for 10 min. The samples were then alternately hand mixed and centrifuged (4000 rpm) until homogeneous by visual inspection (ca. 1–3 cycles of hand mixing and centrifuging). It should be noted that the LLC samples are sensitive to water loss or gain, depending on relative humidity of the laboratory environment. Therefore, special attention was taken to keep the sample vials sealed as much as possible during mixing and transferring to minimize composition drift.

The composition and temperature ranges of the LLC phases formed by the mixtures described above were first determined using variable-temperature PLM

analysis. Samples of various mixture compositions were prepared and then pressed thinly between a glass microscope slide and a coverslip to help minimize composition drift from ambient atmospheric water uptake or solvent evaporation. This sandwiched assembly was then placed on the PLM thermal stage and annealed to 100 °C. The sample was slowly cooled and allowed to return to room temperature. The sample was then heated to 100 °C at a rate of 5 °C/min and its optical texture(s) as a function of temperature and composition were recorded via digital image capture. Images were captured at 50x magnification. Changes in optical texture were used to determine potential changes in the LLC phase of the mixture.

The different phase regions (with PLM images shown) of monomers **1a–f** + 0.1 M aq. NH₄Cl solution (as determined by the PLM procedure described above) are shown in Fig. S15–S20 below. The identity of each observed phase differentiated by PLM analysis was then confirmed quantitatively using ambient-temperature PXRD or SAXS by analyzing a bulk film (ca. 180-μm thick) of a temperature-composition point in each distinct phase region (as elucidated by PLM analysis) that was radically photo-cross-linked to permanently trap the phase nanostructure (see Section V(b)).
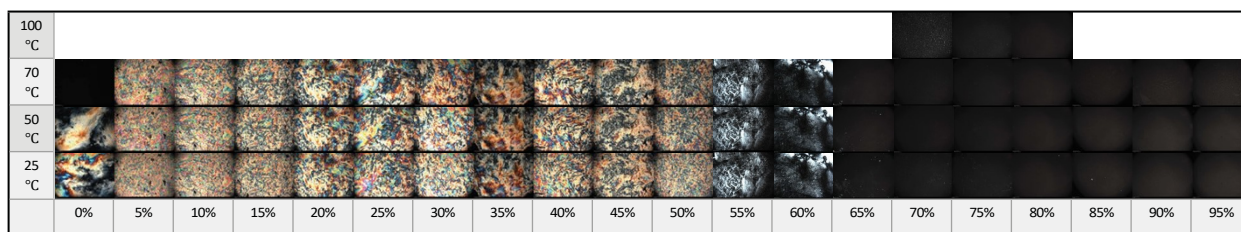
Fig. S15 PLM images (50x mag) used to map the phase regions of monomer **1a** + 0.1 M aq. NH₄Cl determined by variable-temperature PLM analysis, where the y-axis is the temperature of the PLM thermal stage (25–100 °C) and the x-axis is sample composition (0–95 wt.% 0.1 M aq. NH₄Cl solution).
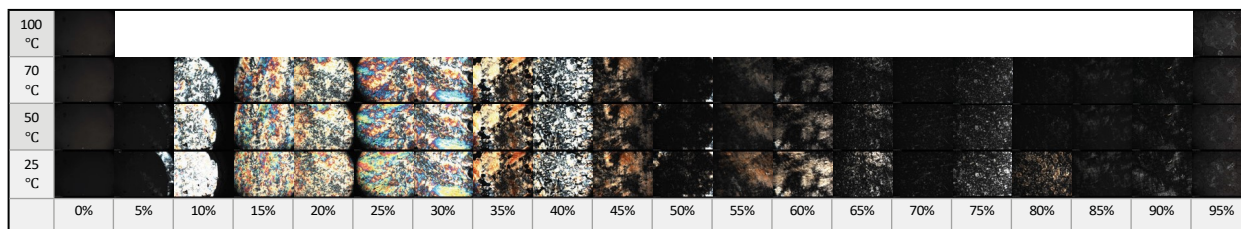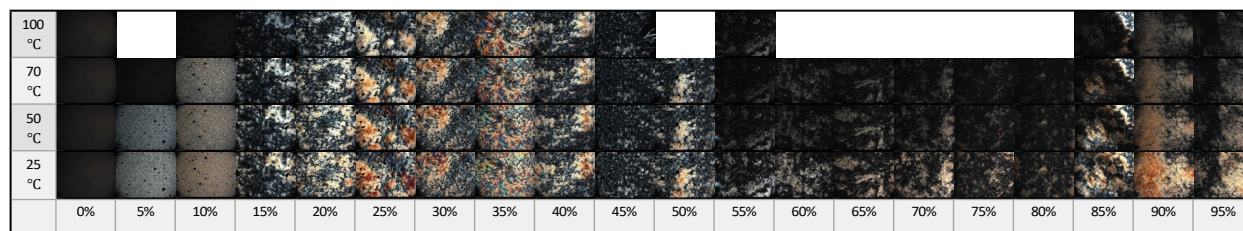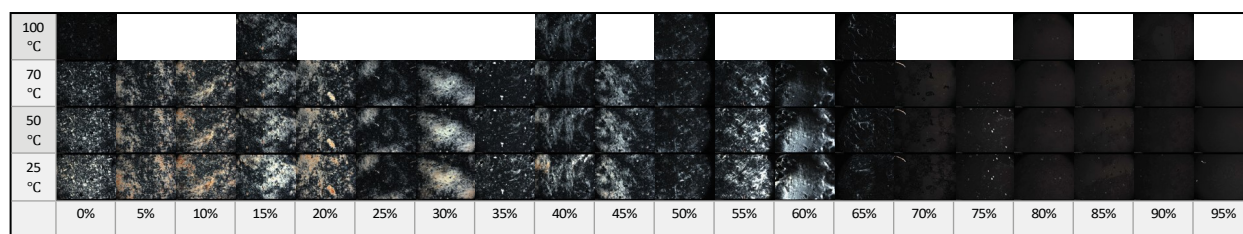

Fig. S16 PLM images (50x mag) used to map the phase regions of monomer **1b** + 0.1 M aq. NH₄Cl determined by variable-temperature PLM analysis, where the y-axis is the temperature of the PLM thermal stage (25–100 °C) and the x-axis is sample composition (0–95 wt.% 0.1 M aq. NH₄Cl solution).
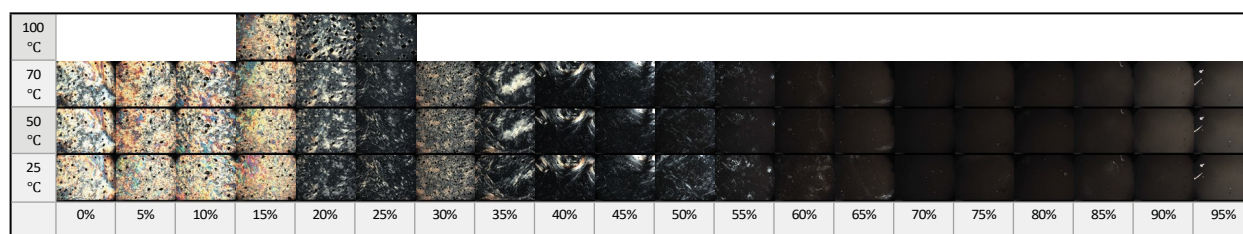
Fig. S17 PLM images (50x mag) used to map the phase regions of monomer **1c** + 0.1 M aq. NH₄Cl determined by variable-temperature PLM analysis, where the y-axis is the temperature of the PLM thermal stage (25–100 °C) and the x-axis is sample composition (0–95 wt.% 0.1 M aq. NH₄Cl solution).
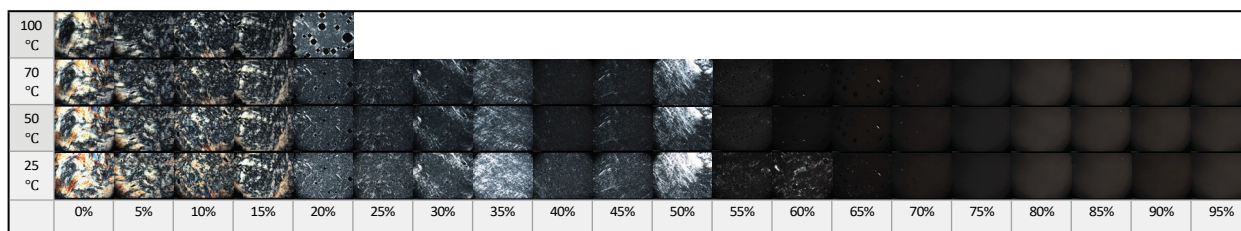

Fig. S18 PLM images (50x mag) used to map the phase regions of monomer **1d** + 0.1 M aq. NH₄Cl determined by variable-temperature PLM analysis, where the y-axis is the temperature of the PLM thermal stage (25–100 °C) and the x-axis is sample composition (0–95 wt.% 0.1 M aq. NH₄Cl solution).

Fig. S19 PLM images (50x mag) used to map the phase regions of monomer **1e** + 0.1 M aq. NH₄Cl determined by variable-temperature PLM analysis, where the y-axis is the temperature of the PLM thermal stage (25–100 °C) and the x-axis is sample composition (0–95 wt.% 0.1 M aq. NH₄Cl solution).

Fig. S20 PLM images (50x mag) used to map the phase regions of monomer **1f** + 0.1 M aq. NH$_4$Cl determined by variable-temperature PLM analysis, where the y-axis is the temperature of the PLM thermal stage (25–100 °C) and the x-axis is sample composition (0–95 wt.% 0.1 M aq. NH$_4$Cl solution).

Note: Some images of samples at 100 °C were not captured due to solvent evaporation.

(b) Cross-linked bulk film fabrication & quantitative phase identification by PXRD and SAXS analyses

Bulk (ca. 180-µm-thick) cross-linked films of monomers **1a–f** + 0.1 M aq. NH$_4$Cl solution with compositions in each phase region to be identified were made as follows: The appropriate amounts of monomer **1a–f** and 0.1 M aq. NH$_4$Cl solution as well as 1 wt.% 2-hydroxy-2-methylpropiophenone (HMP, a radical photo-initiator) were added to a tared glass vial to target a temperature-composition point in each distinct phase region (as elucidated by PLM analysis). The vial was sealed with the corresponding cap and centrifuged at 4000 rpm for 10 min. The sample was then alternately hand mixed and centrifuged (4000 rpm) until homogeneous by visual inspection (ca. 1–3 cycles of hand mixing and centrifuging). The tacky paste was placed between Mylar® sheets with coverslip spacers in each corner (to minimize composition drift due to ambient atmospheric water uptake or solvent evaporation) and annealed (70 °C for 1–2 min) between two 6" x 6" fused silica plates that were squeezed together by four clamps. The Mylar® sheet/film sandwich was removed from the plates and was put on the bench for 10 min to cool to room temperature. It was then returned to the fused silica plate assembly, heated to the desired temperature (as necessary), and irradiated with 365-nm UV light with an intensity of >1 mW/cm^2 at the sample surface for 1 h to radically cross-link.

Room-temperature PXRD spectra of the resulting cross-linked bulk film samples of the monomers were taken in the Gin laboratory at the University of Colorado Boulder in the open air using a custom-made, clamped sandwich-type film holder with a central open window. The clamped polymer film was then positioned such that the open face of the film was directly in the path of the X-ray beam, between the beam source and the detector (i.e., through-film transmission mode). The *d*-spacing pattern of the PXRD peaks was used to quantitatively identify the type of LLC phase formed at the exact temperature-composition point used to form the cross-linked sample, so long as more than one PXRD peak were present to clearly index an LLC phase with a specific geometry.[2] Bulk cross-

linked film samples were also characterized by SAXS at the University of Pennsylvania. The bulk film samples were stuck onto the standard sample holder by Kapton tape and positioned in the path of the X-ray beam. All 2D scattering signals were integrated into 1D plots of scattering intensity (I) versus q by the Foxtrot software.

An ideal, symmetric illustration of the various phase regions and the different LLC phases typically observed in amphiphile-water mixtures is shown in Fig. S21, below.[4] However, not all amphiphile-solvent systems exemplify every phase, and experimental phase diagrams are generally not as symmetric in nature.
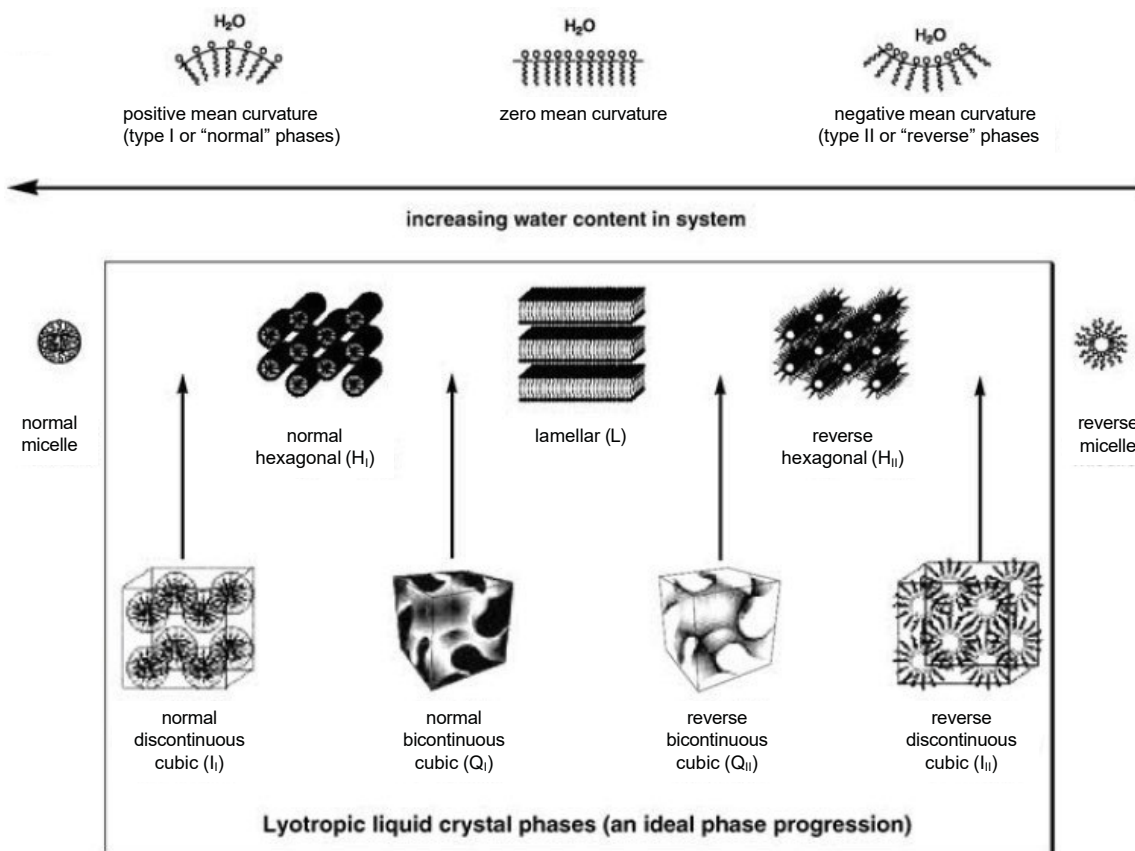
Fig. S21 Schematic representations of the most common LLC phases formed by amphiphiles in water in an ideal phase progression, with a focus on the Q phases. (Partially reproduced from Ref. 4 with permission. Copyright Nature Publishing Group, 2012.)

As previously discussed, preliminary assignment of LLC phase regions was done by qualitatively assessing the changes in PLM optical texture; specifically, determining if the texture was black or birefringent. PXRD and SAXS analyses can be used to quantitatively confirm LLC phase regions in the following manner:

If the optical texture was black and the PXRD or SAXS spectrum of the corresponding cross-linked bulk film had a broad/weak principal peak or effectively no sharp diffraction peaks, then the phase region was categorized as an amorphous isotropic

phase (Iso) (i.e., an amorphous melt or unordered collection of normal or reverse spherical micelles).[2,5] If the PLM optical texture was birefringent and the PXRD and SAXS spectra of the corresponding cross-linked bulk film exhibited a single or multiple sharp diffraction peaks, then the observed phase was assigned as hexagonal (H), lamellar (L), or an unidentified anisotropic phase or mixture of unidentified anisotropic phases (Unidentified anisotropic phase(s)).[2,5] H phases have PXRD diffraction peaks with a *d*-spacing pattern of $1 : 1/\sqrt{3} : 1/\sqrt{4} : 1/\sqrt{7} : 1/\sqrt{9}$ … etc. with respect to the principal peak, corresponding to SAXS peaks at scattering vectors with the ratios $1 : \sqrt{3} : \sqrt{4} : \sqrt{7} : \sqrt{9}$ … etc.[2,5] L phases have PXRD diffraction peaks with a *d*-spacing pattern of $1 : 1/2 : 1/3 : 1/4 : 1/5$ … etc. with respect to the principal peak, corresponding to SAXS peaks at scattering vectors with the ratios $1 : 2 : 3 : 4 : 5$ … etc.[2,5] If the PXRD and SAXS spectra showed peaks that could not be clearly indexed to those of H or L phases, but the presence of a sharp peak or peaks suggested some degree of order, then the phase was assigned as Unidentified anisotropic phase(s).[2,5] Assignment of bicontinuous cubic (Q) phase regions was done by confirming the presence of a black, pseudo-isotropic optical texture (a consequence of the cubic symmetry when subjected to polarized light) and well-defined order.[2] Q phases typically exhibit PXRD diffraction peaks with a *d*-spacing pattern of $1/\sqrt{6} : 1/\sqrt{8} : 1/\sqrt{14} : 1/\sqrt{16} : 1/\sqrt{18} : 1/\sqrt{20}$ for double gyroid ($Ia\bar{3}d$) or $1/\sqrt{2} : 1/\sqrt{3} : 1/\sqrt{4} : 1/\sqrt{6} : 1/\sqrt{8} : 1/\sqrt{9}$ for $Pm\bar{3}m$ with respect to the principal peak, corresponding to SAXS diffraction peaks at particular ratios of scattering vectors (e.g., $\sqrt{6} : \sqrt{8} : \sqrt{14} : \sqrt{16} : \sqrt{18} : \sqrt{20}$ for double gyroid ($Ia\bar{3}d$) or $\sqrt{2} : \sqrt{3} : \sqrt{4} : \sqrt{6} : \sqrt{8} : \sqrt{9}$ for $Pm\bar{3}m$).[2,4,5] Q phases are optically transparent but are typically very viscous in nature because they consist of 3D-interpenetrating hydrophobic and hydrophilic channels.[2,4,5]

In addition, each H or Q phase with the specific geometry/symmetry described above can also be sub-classified in terms of whether the hydrophilic−hydrophobic interface curves away from (i.e., type I, normal) or toward the aqueous regions (i.e., type II, reverse).[2,5] To unequivocally determine whether an observed LLC phase is type I or type II, an L phase needs to be present in the phase diagram as a central reference point that has no preferred net curvature towards either the hydrophilic or hydrophobic domains.[2,5] Then, LLC phases on the water (or polar solvent)-excessive side of the L phase can be assigned as type I (i.e., normal), and those on the water (or polar solvent)-deficient side can be assigned as type II (i.e., reverse).[5] Therefore, it can be concluded that the H and Q phases seen for monomers **1b**, **1c**, **1e**, and **1f** + 0.1 M aq. NH₄Cl solution are all type II, as they lie on the water-deficient side of the L phase in each monomer's case; whereas monomers **1a** and **1d** only contain unidentified anisotropic phase(s).

*Note: It was not possible to identify the unit cell geometry of the Q_II phases formed by monomers **1b** and **1c** from the PXRD or SAXS spectra. PXRD and SAXS studies were not able to resolve enough diffraction peaks in the Q-phase samples to unequivocally identify the type of unit cell. However, $Ia\bar{3}d$ and $Pn\bar{3}m$ space groups are frequently observed for Q LLC phases reported in literature and we speculate that the systems here correspond to one of those.[5]*

Some example PXRD spectra and PLM images used for phase assignments are shown in Fig. S22 and S23, below, while the rest of the PXRD and SAXS data for all phase regions of monomers **1a–f** are compiled in Section VIII.
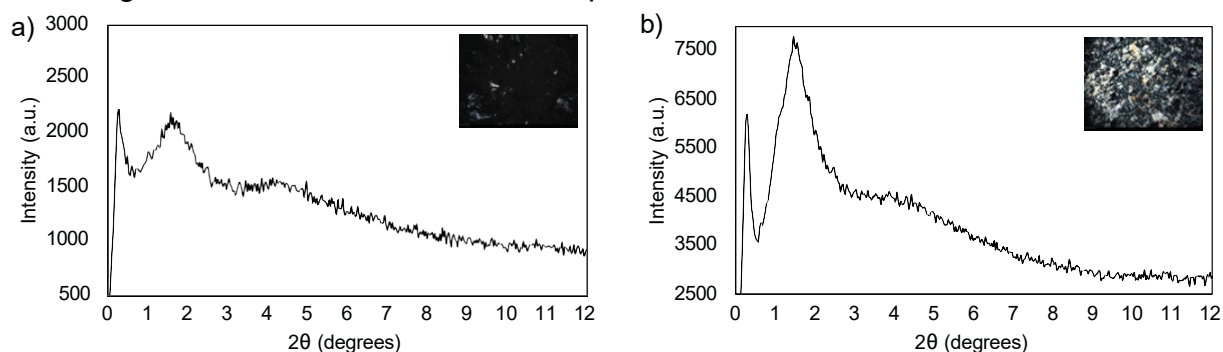

Fig. S22 Example PXRD profiles and PLM images (50x mag) used to assign phases in the partial phase diagrams: a) a disordered isotropic (Iso) phase obtained from a polymerized mixture of 30:70:1 (w/w/w) monomer **1a**/0.1 M aq. NH_4Cl/HMP at 60 °C, and b) an unidentified anisotropic phase or mixture of phases obtained from a polymerized mixture of 72.5:27.5:1 (w/w/w) monomer **1a**/0.1 M aq. NH_4Cl/HMP at 25 °C.
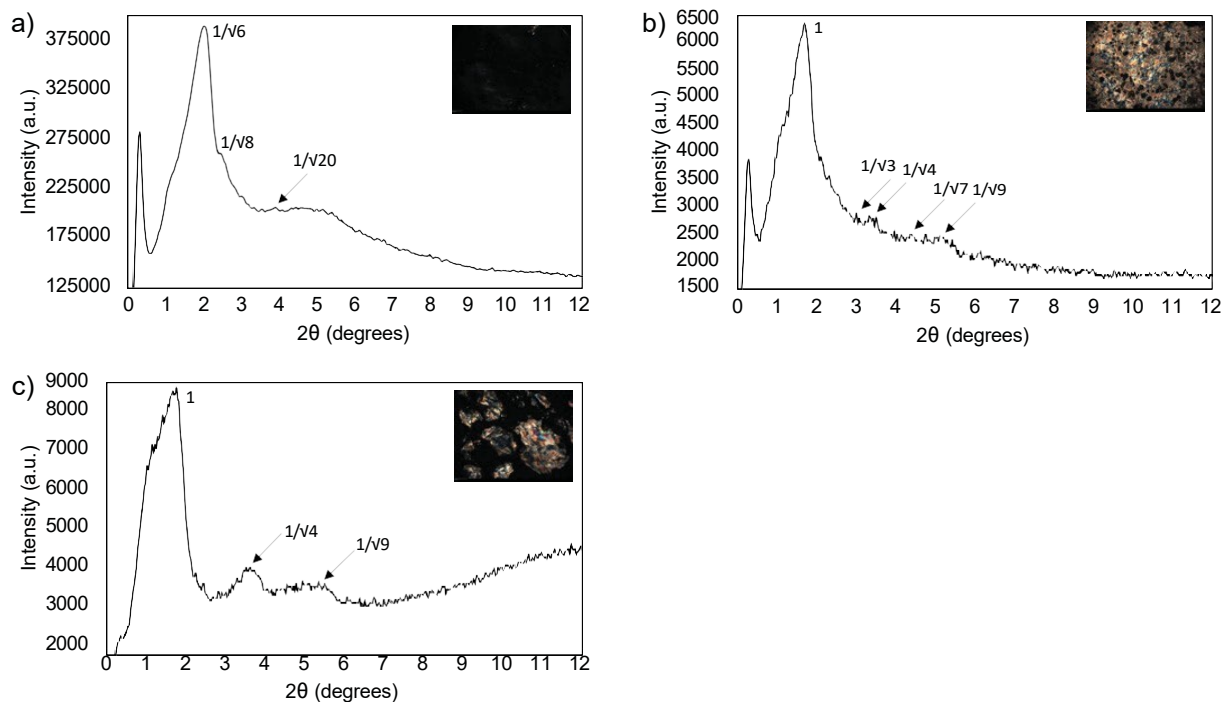
Fig. S23 Example PXRD profiles and PLM images (50x mag) of LLC phases formed by monomer **1b** with 0.1 M aq. NH_4Cl solution: a) a type II bicontinuous cubic (Q_{II}) phase obtained from a polymerized mixture of 95:5:1 (w/w/w) monomer **1b**/0.1 M aq. NH_4Cl/HMP at 70 °C, b) a type II hexagonal (H_{II}) phase obtained from a polymerized

mixture of 75:25:1 (w/w/w) monomer **1b**/0.1 M aq. NH₄Cl/HMP at 25 °C, and c) the lamellar (L) phase obtained from a polymerized mixture of 47.5:52.5:1 (w/w/w) monomer **1b**/0.1 M aq. NH₄Cl/HMP at 25 °C.

Using the combined PLM, PXRD, or SAXS methods and the criteria detailed above, complete phase diagrams of the six phosphobetaine-based zwitterionic monomers **1a–f** with added 0.1 M aq. NH₄Cl solution were finalized (see Fig. S24).
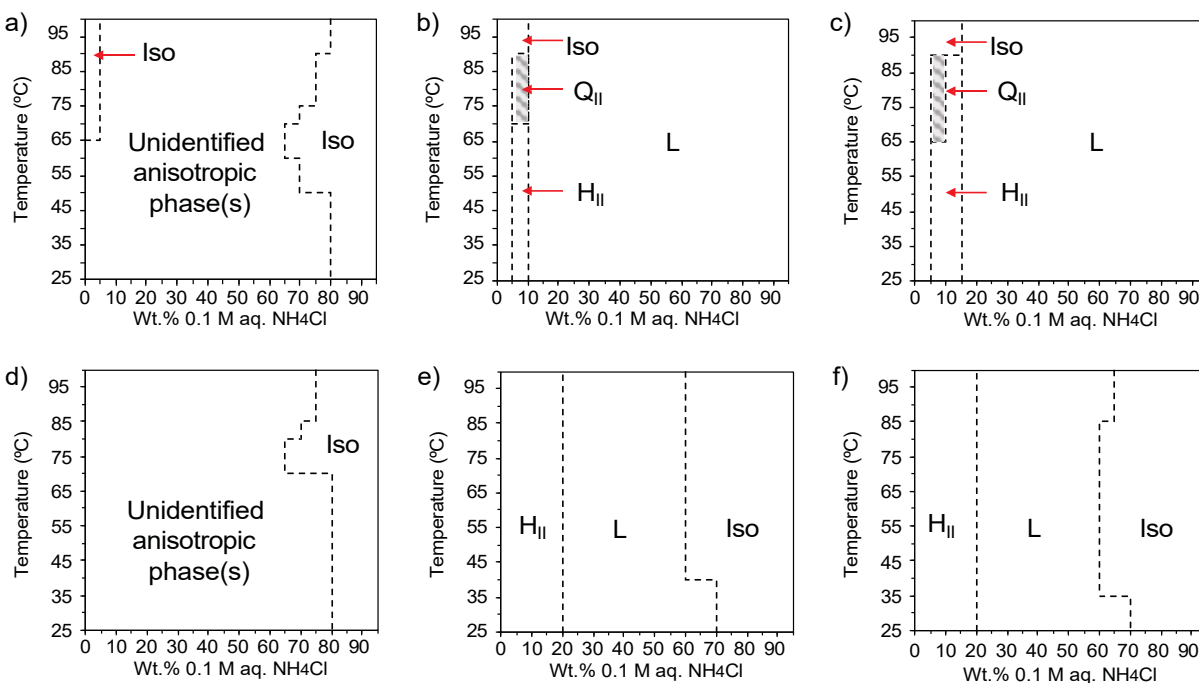

Fig. S24 Phase diagrams of monomers **1a–f** with 0.1 M aq. NH₄Cl solution: a) **1a**; b) **1b**; c) **1c**; d) **1d**; e) **1e**; and f) **1f**. Iso = amorphous isotropic phase (i.e., no order by PXRD/SAXS); Q$_{II}$ = type II bicontinuous cubic phase; H$_{II}$ = type II hexagonal phase; and L = lamellar phase. Heterogeneous regions omitted. Note: data compiled at Boulder, CO (altitude = 5328 ft, ambient pressure = ca. 623 torr); values may be slightly different at other locations.

*Note: Although each monomer (i.e., **1a–f**) demonstrated the potential to form a Q phase with 0.1 M aq. NH₄Cl by preliminary PLM-based solvent-penetration scan analysis (see Table S1), more-detailed and careful systematic PLM composition and temperature analysis (during full phase diagram elucidation) revealed that only monomers **1b** and **1c** displayed completely black optical textures. The lack of a black optical texture during the detailed PLM analysis of the other four monomers implied that a pure Q phase was not present. We hypothesize that the lack of a Q phase for monomers **1a**, **1d**, **1e**, and **1f** may be related to the zwitterionic headgroup size and shape (i.e., bulk), which is discussed in the manuscript.*

VI. Example FT-IR Spectra for Determining the Extent of Polymerization in Radically Photo-cross-linked Q-phase Samples
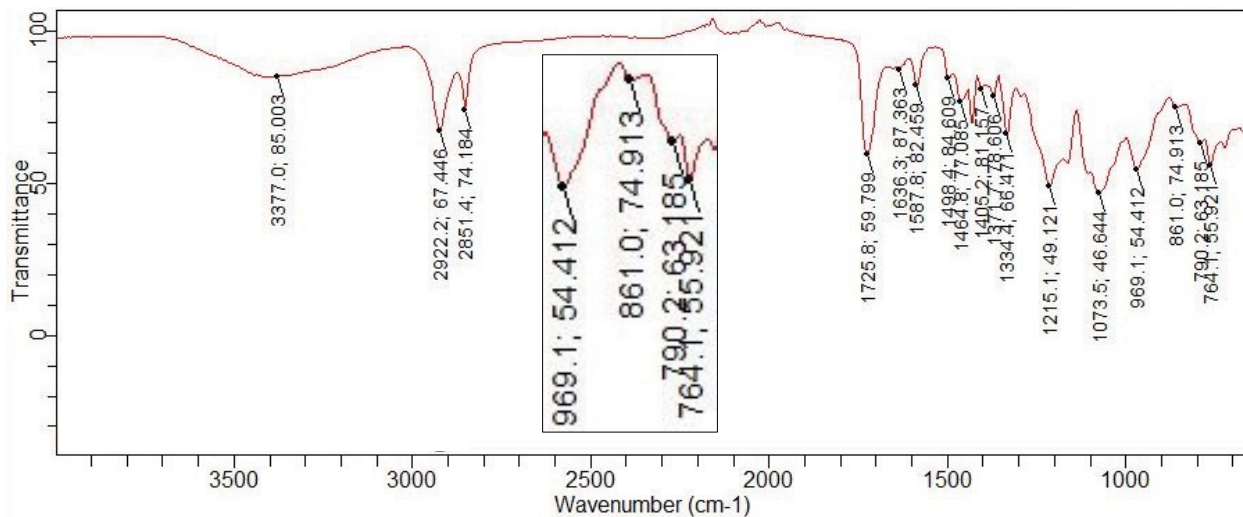

Fig. S25 Sample FT-IR spectrum of a sample made of 95:5:1 (w/w/w) monomer **1b**/0.1 M aq. NH₄Cl solution/HMP after photopolymerization at 70 °C. Inset: Zoomed-in region of interest for monitoring the polymerizable group conversion. Note the absence of an acrylate C=C stretching band at 812 cm⁻¹.
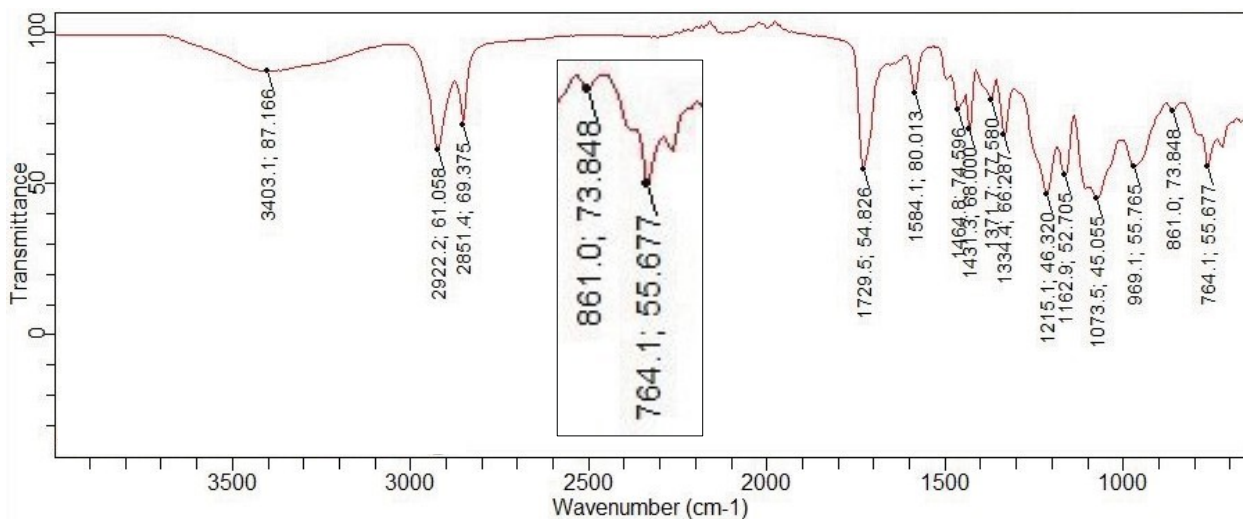

Fig. S26 Sample FT-IR spectrum of a sample made of 95:5:1 (w/w/w) monomer **1c**/0.1 M aq. NH₄Cl solution/HMP after photopolymerization at 70 °C. Inset: Zoomed-in region of interest for monitoring the polymerizable group conversion. Note the absence of an acrylate C=C stretching band at 812 cm⁻¹.

VII. Example DSC Spectra for Characterization of Water Molecules in the System

DSC measurements of the unpolymerized Q_{II}-phase LLC mixtures of **1b** and **1c** and their corresponding cross-linked Q_{II} bulk polymer films were taken to see if freezing-bound or non-freezing-bound water molecules could be identified in the samples. As can be seen in Fig. S27, no phase transition of water was observed for these Q-phase nanostructured materials. Therefore, it was not possible to identify freezing-bound water or non-freezing-bound water in the samples.
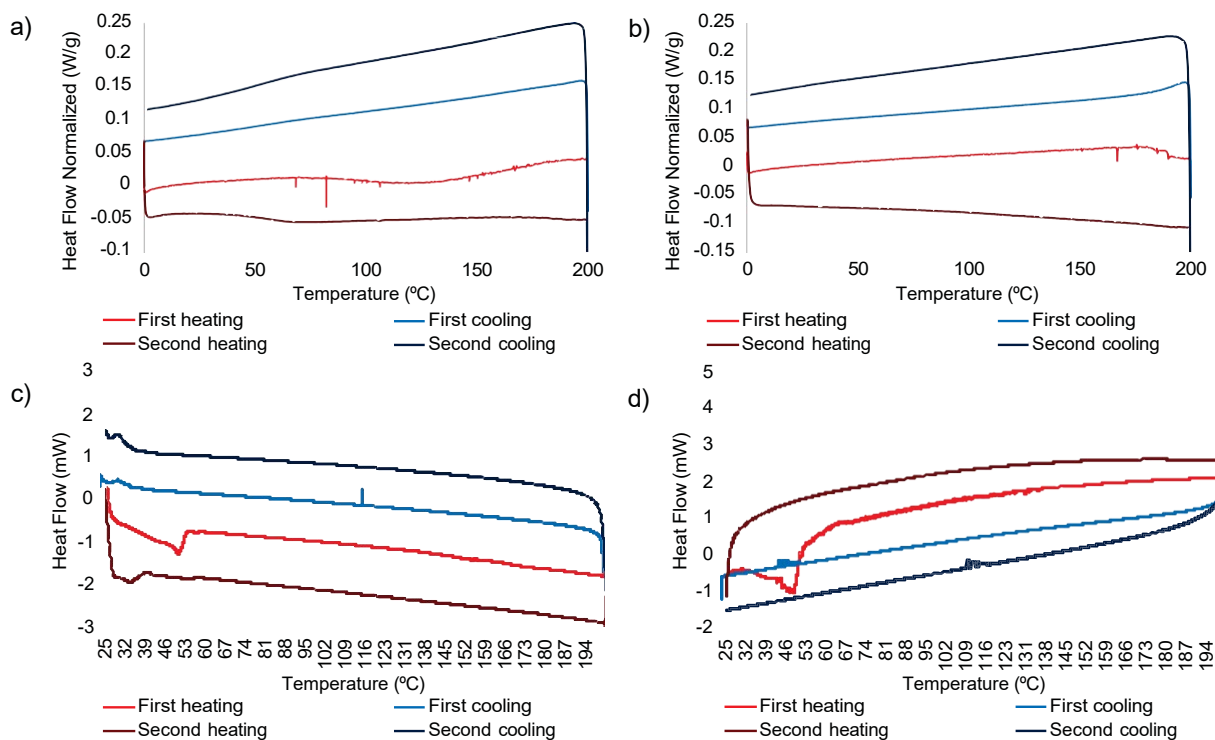
Fig. S27 DSC spectra of samples made of a) 95:5:1 (w/w/w) monomer **1b**/0.1 M aq. NH$_4$Cl solution/HMP and b) 95:5:1 (w/w/w) monomer **1c**/0.1 M aq. NH$_4$Cl solution/HMP after photopolymerization at 70 °C; and c) 95:5 (w/w) monomer **1b**/0.1 M aq. NH$_4$Cl solution and d) 95:5 (w/w) monomer **1c**/0.1 M aq. NH$_4$Cl solution before photopolymerization.

VIII. **Example PXRD and SAXS Spectra for All Phase Regions of Monomers 1a–f + 0.1 M aq. NH₄Cl Solution via Analysis of Radically Photo-Cross-Linked Samples from the Phase Regions**
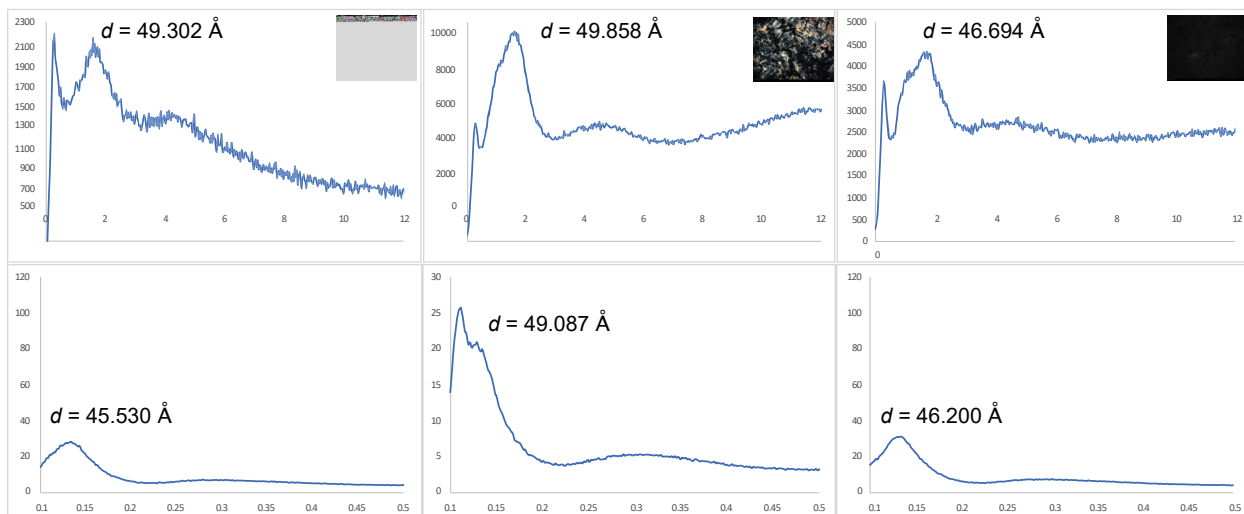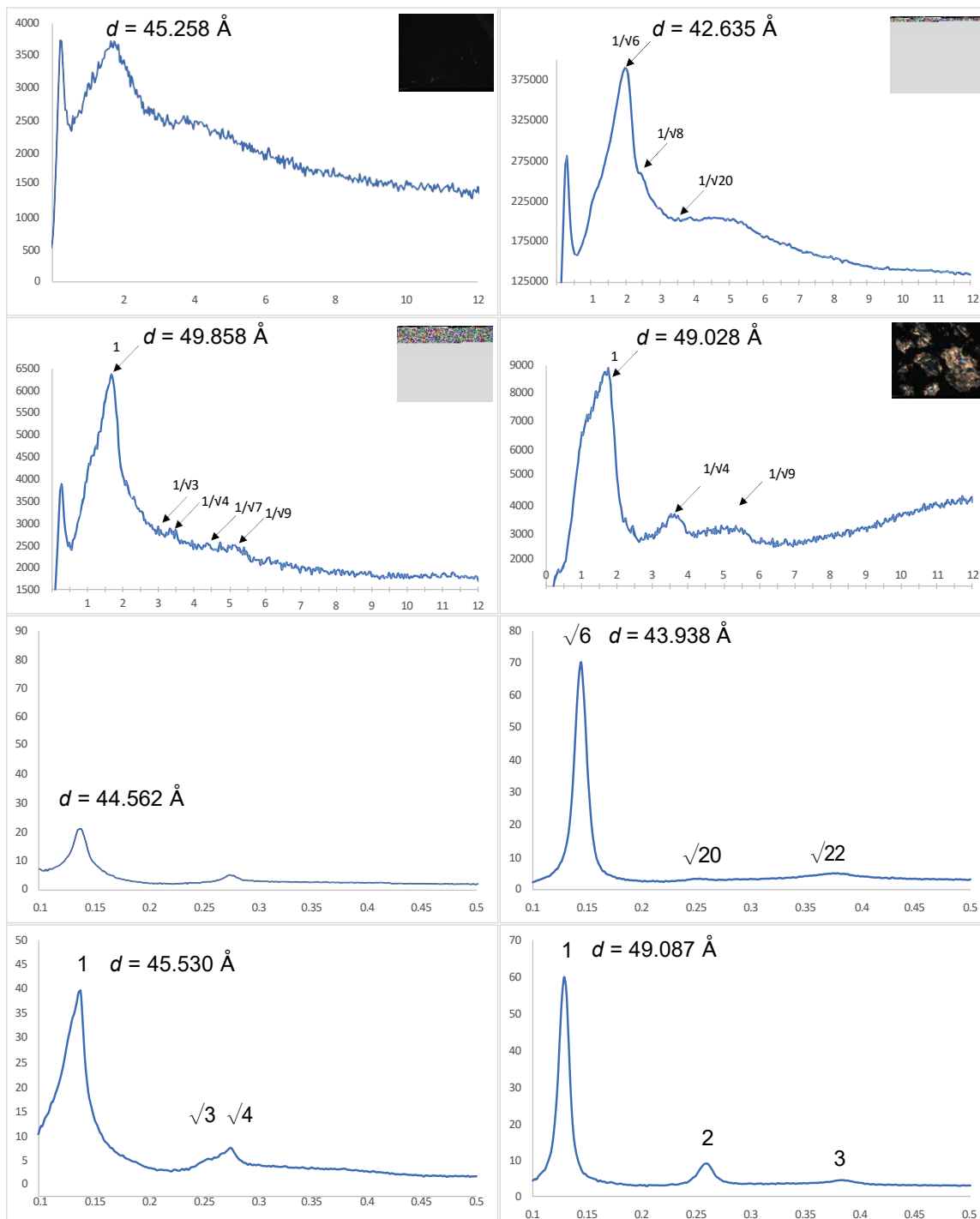

Fig. S28 PXRD (above) profiles, SAXS (below) profiles, and PLM images (50x mag) used to assign regions in phase diagrams obtained from polymerized mixtures of monomer **1a**/0.1 M aq. NH₄Cl/HMP: (left) a disordered isotropic (Iso) phase (100:0:1 (w/w/w) at 83 °C), (middle) an unidentified anisotropic phase or mixture of phases (72.5:27.5:1 (w/w/w) at 25 °C), and (right) a disordered isotropic (Iso) phase (30:70:1 (w/w/w) at 60 °C).
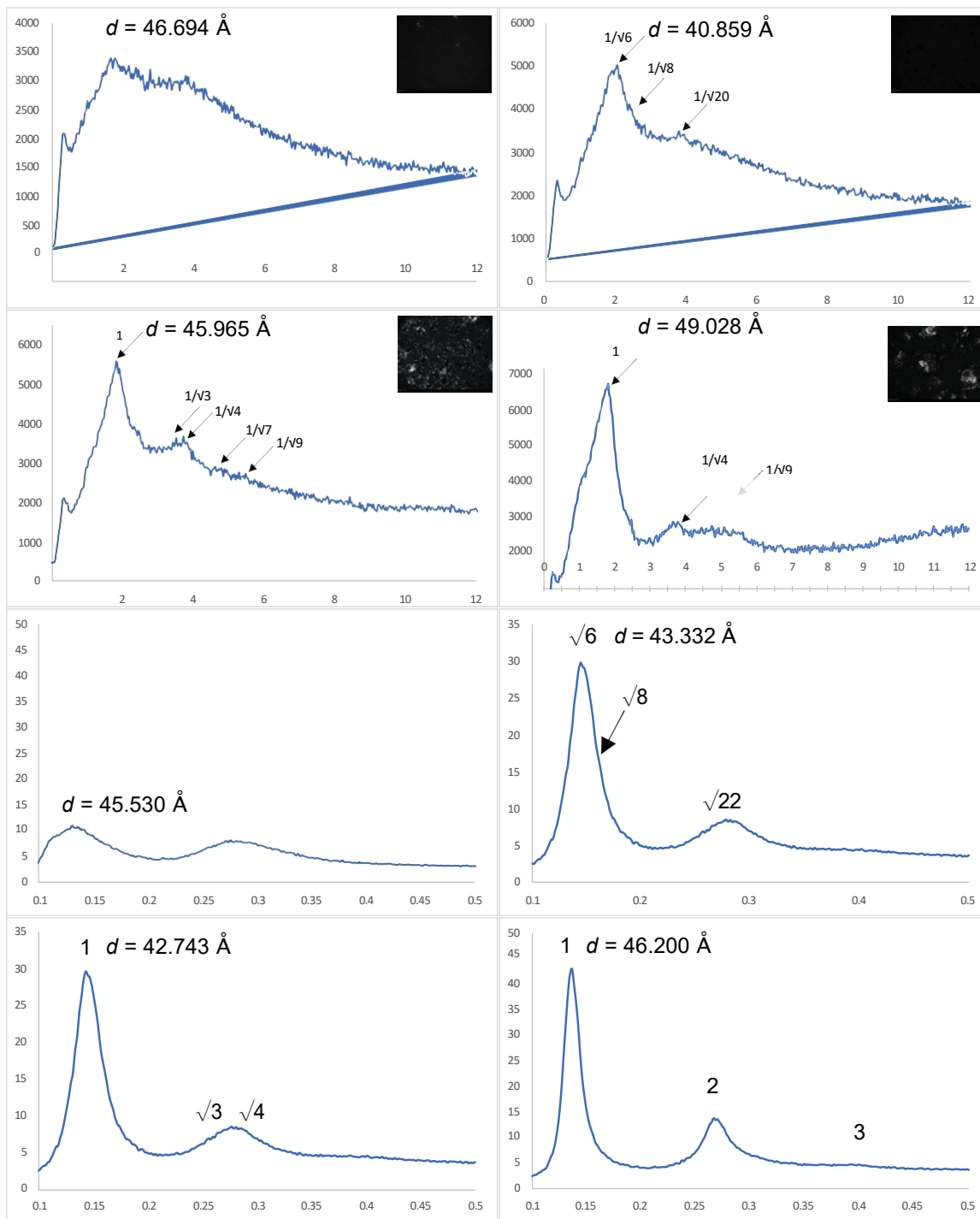
Fig. S29 PXRD (above) profiles, SAXS (below) profiles, and PLM images (50x mag) used to assign regions in phase diagrams obtained from polymerized mixtures of monomer **1b**/0.1 M aq. NH$_4$Cl/HMP: (upper left) a disordered isotropic (Iso) phase (100:0:1 (w/w/w) at 83 °C), (upper right) a type II bicontinuous cubic (Q$_{II}$) phase (95:5:1 (w/w/w) at 70 °C), (lower left) a type II hexagonal (H$_{II}$) phase (95:5:1 (w/w/w) at 25 °C), and (lower right) a lamellar (L) phase (47.5:52.5:1 (w/w/w) at 25 °C).
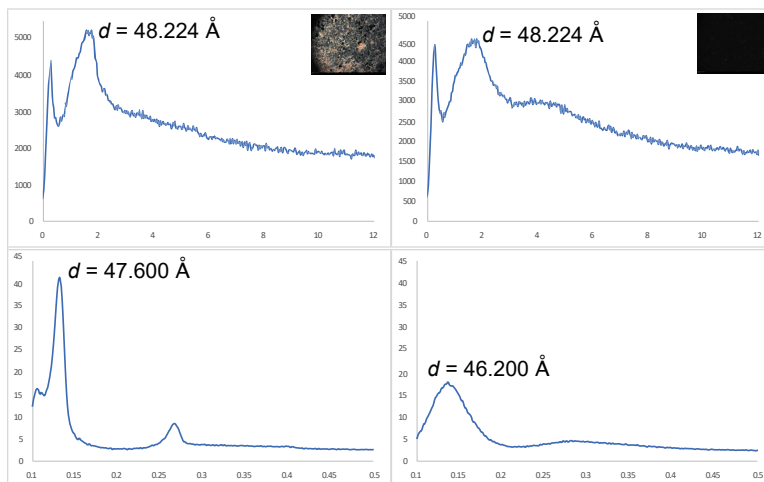
Fig. S30 PXRD (above) profiles, SAXS (below) profiles, and PLM images (50x mag) used to assign regions in phase diagrams obtained from polymerized mixtures of monomer **1c**/0.1 M aq. NH_4Cl/HMP: (upper left) a disordered isotropic (Iso) phase (100:0:1 (w/w/w) at 83 °C), (upper right) a type II bicontinuous cubic (Q_{II}) phase (95:5:1 (w/w/w) at 70 °C), (lower left) a type II hexagonal (H_{II}) phase (92.5:7.5:1 (w/w/w) at 25 °C), and (lower right) a lamellar (L) phase (67.5:32.5:1 (w/w/w) at 25 °C).

Fig. S31 PXRD (above) profiles, SAXS (below) profiles, and PLM images (50x mag) used to assign regions in phase diagrams obtained from polymerized mixtures of monomer **1d**/0.1 M aq. NH₄Cl/HMP: (left) an unidentified anisotropic phase or mixture of phases (75:25:1 (w/w/w) at 25 °C), and (right) a disordered isotropic (Iso) phase (30:70:1 (w/w/w) at 70 °C).
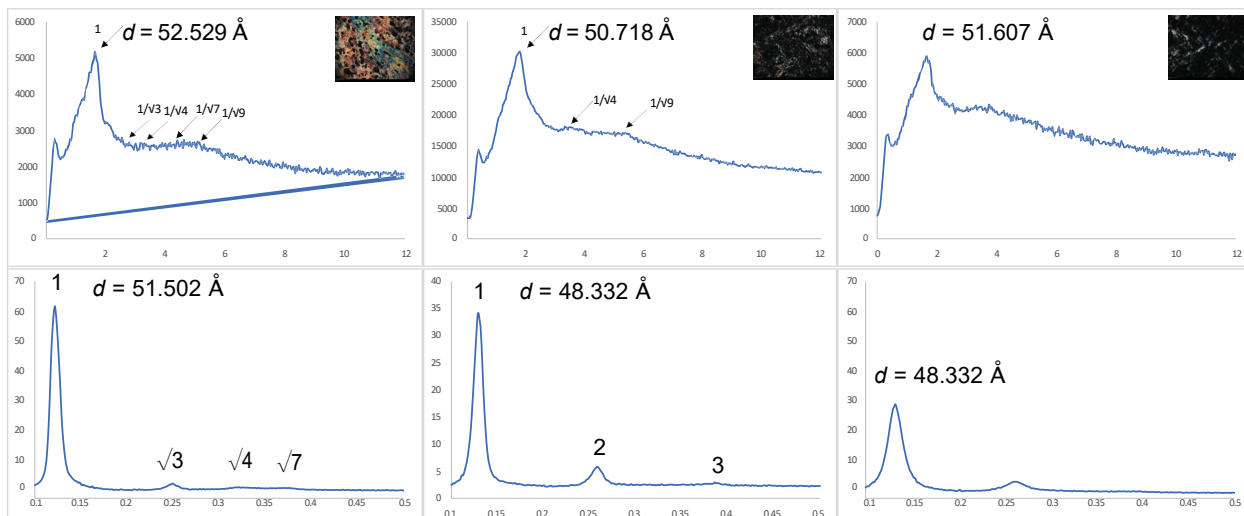

Fig. S32 PXRD (above) profiles, SAXS (below) profiles, and PLM images (50x mag) used to assign regions in phase diagrams obtained from polymerized mixtures of monomer **1e**/0.1 M aq. NH₄Cl/HMP: (left) type II hexagonal (H$_{II}$) phase (90:10:1 (w/w/w) at 25 °C), (middle) a lamellar (L) phase (75:25:1 (w/w/w) at 25 °C), and (right) a disordered isotropic (Iso) phase (40:60:1 (w/w/w) at 70 °C).
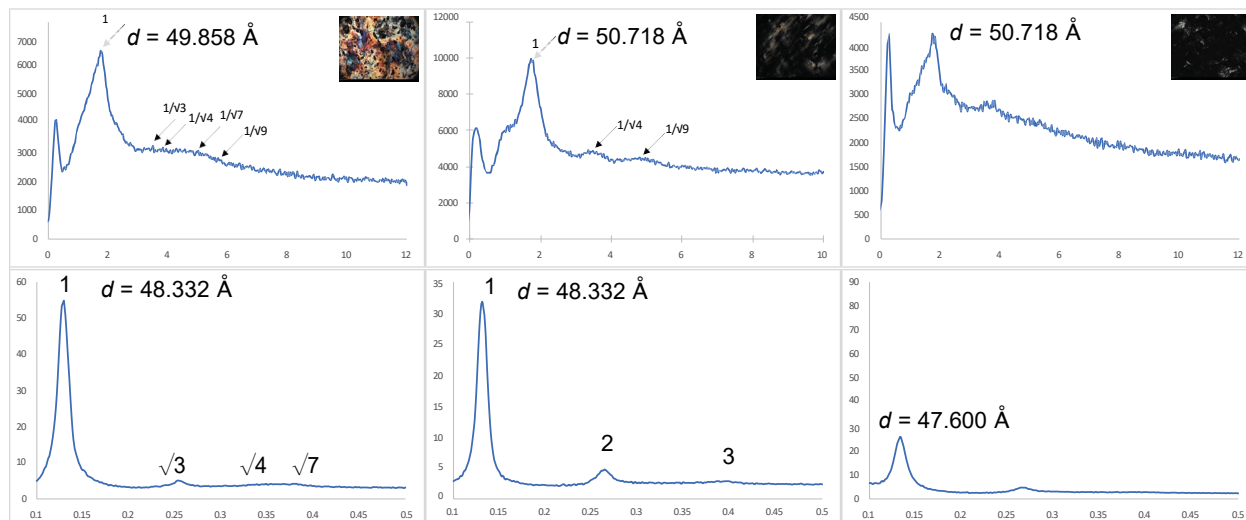
Fig. S33 PXRD (above) profiles, SAXS (below) profiles, and PLM images (50x mag) used to assign regions in phase diagrams obtained from polymerized mixtures of monomer **1f**/0.1 M aq. NH$_4$Cl/HMP: (left) type II hexagonal (H$_{II}$) phase (90:10:1 (w/w/w) at 25 °C), (middle) a lamellar (L) phase (62.5:37.5:1 (w/w/w) at 25 °C), and (right) a disordered isotropic (Iso) phase (40:60:1 (w/w/w) at 70 °C).

IX. Preliminary TFC Q$_{II}$ Polymer Membrane Fabrication Studies & Characterization

TFC polymer membranes of **1b** and **1c** were fabricated on ultraporous PES support membranes using a blade-casting approach similar to another LLC thin-film solution-processing procedure reported in the literature.[6] Firstly, **1b** or **1c** mixtures consisting of monomer/0.1 M aq. NH$_4$Cl/HMP (95:5:1 (w/w/w)) were prepared as 20 wt.% solutions in methanol. The solutions were filtered through a 0.22-µm PVDF syringe filter to remove any potential small, cross-linked pieces or dust particles. The PES support membranes were soaked in methanol for 30 min to remove any preservatives or wetting agents before coating. Then, a film-casting doctor blade set to 40-µm height was used to evenly coat the solution onto the PES support membrane. The PES support membrane was taped to a clean flat surface in a square-like fashion. Approximately 0.6 mL of the casting solution was pipetted along the length of the blade sitting at the edge of the taped support, and it was then immediately drawn across the support surface at a slow constant speed. The coated membrane sample was allowed to air dry at ambient temperature for 30 min. This casting procedure was repeated by drawing the doctor blade in the opposite direction of the initial cast to achieve uniform distribution of material, and again, allowed to air dry for 30 min at ambient temperature. A hotplate was warmed to 70 °C and the coated membrane sample was placed atop for 5 min and then allowed to cool back to ambient temperature. This quick heating process was performed to remove excess methanol casting solvent and to anneal the sample while attempting to minimize solvent

evaporation. Lastly, the TFC membrane sample was photopolymerized under 365-nm light for 1 h at 70 °C.

The presence and thickness of the polymer coating was confirmed by SEM imaging at the University of Pennsylvania. The sample membrane was cut by a razor blade and stood on the sample stage for characterization of the cross-sectional area (see Fig. S34). A dense, thin polymer film was successfully coated onto the PES support and found to be ca. 6.4 μm thick. The degree of polymerization and retention of the Q_{II} nanostructure for the TFC membrane was characterized by FT-IR spectroscopy and SAXS analysis (see Fig. S35 and Fig. S36, respectively) at the University of Pennsylvania.
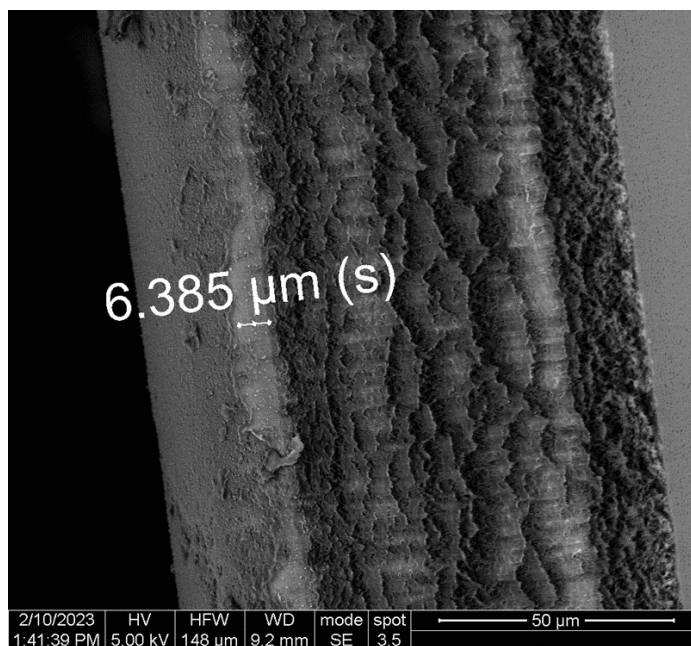

Fig. S34 Sample SEM cross-section photograph of a thin film coated onto a PES support membrane made of 95:5:1 (w/w/w) monomer **1b**/0.1 M aq. NH_4Cl solution/HMP after photopolymerization at 70 °C.
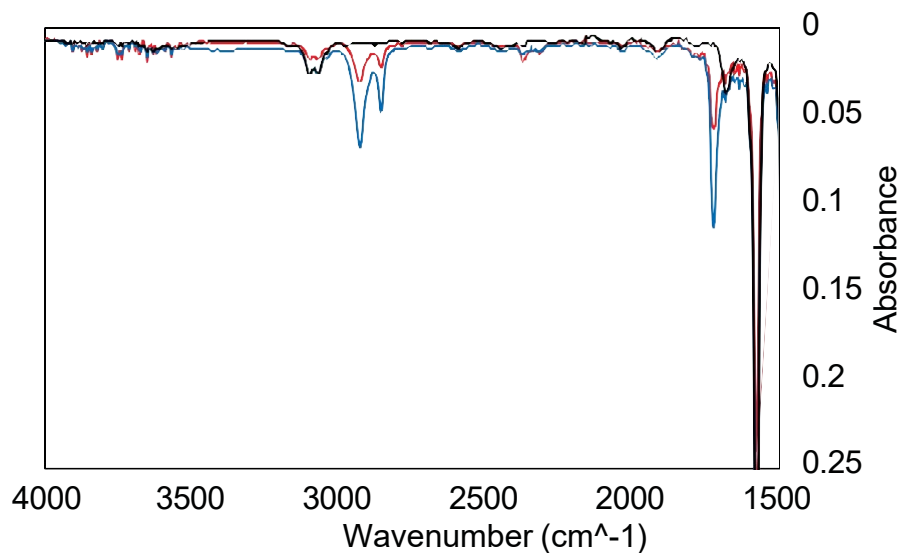
Fig. S35 Sample FT-IR spectrum of a supported thin-film sample made of 95:5:1 (w/w/w) monomer **1b**/0.1 M aq. NH$_4$Cl solution/HMP pre- (red) and post-photopolymerization (blue) at 70 °C on a PES support membrane (black).
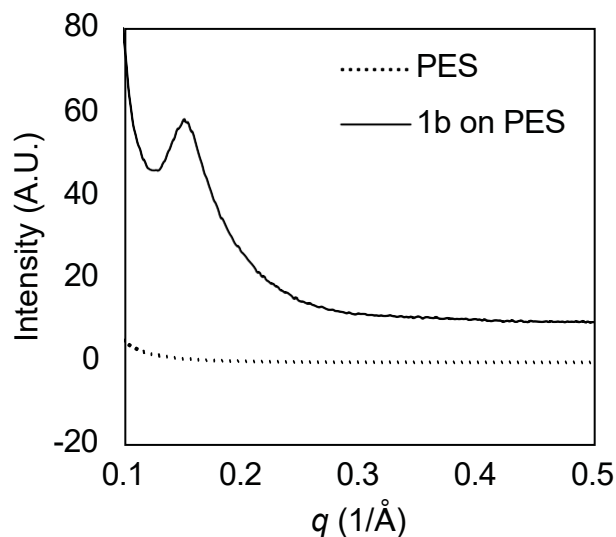

Fig. S36 SAXS spectra of a TFC sample made of 95:5:1 (w/w/w) monomer **1b**/0.1 M aq. NH$_4$Cl solution/HMP after photopolymerization at 70 °C on a PES support film, confirming retention of the initial Q$_{II}$ phase after fabrication and photopolymerization. Note that the intensity of the diffraction peaks has diminished compared to PXRD/SAXS of a bulk film sample due to the extreme thinness of the top layer on the composite membrane.

24th August 2023 - Note added after first publication: This Supplementary Information file replaces that originally published 16th May 2023.

X.   References for the Electronic Supplementary Information

(1)   O. Q. Imran, N. K. Kim, L. N. Bodkin, G. E. Dwulet, X. Feng, K. Kawabata, M. Elimelech, D. L. Gin and C. O. Osuji, *Adv. Mater. Interfaces,* 2021, **8**, 2001977.

(2)   P. Li, M. I. Reinhardt, S. S. Dyer, K. E. Moore, O. Q. Imran and D. L. Gin, *Soft Matter*, 2021, **17**, 9259.

(3)   R. Hoffman, *COSY*, accessed 29 Nov. 2022, http://chem.ch.huji.ac.il/nmr/techniques/2d/cosy/cosy.html.

(4)   B. R. Wiesenauer and D. L. Gin, *Polym. J.*, 2012, **44**, 461.

(5)   For general reviews on LLC phases and their classifications, see: (*a*) M. W. Tate, E. F. Eikenberry, D. C. Turner, E. Shyamsunder and S. M. Gruner, *Chem. Phys. Lipids*, 1991, **57**, 147. (*b*) J. M. Seddon, *Biochim. Biophys. Acta*, 1990, **1031**, 1. (*c*) G. J. T. Tiddy, *Phys. Rep.*, 1980, **57**, 1.

(6)   B. M. Carter, B. R. Wiesenauer, R. D. Noble and D. L. Gin, *J. Membr. Sci.*, 2014, **455**, 143.